Sustainable Energy, Grids and Networks 40 (2024) 101545

Contents lists available at ScienceDirect

Sustainable Energy, Grids and Networks

journal homepage: www.elsevier.com/locate/segan

Optimal design model for a public-private Renewable Energy Community in a small Italian municipality

Bruno Laurini [a,*], Barbara Bonvini [b], Stefano Bracco [b]

[a] Department of Wind and Energy Systems, Technical University of Denmark, Kgs. Lyngby 2800, Denmark
[b] Electrical, Electronics and Telecommunication Engineering and Naval Architecture Department (DITEN), University of Genoa, Via Opera Pia 11a, Genoa 16145, Italy

ARTICLE INFO

Keywords:
Renewable energy community
Optimal design
MILP model
Shared energy

ABSTRACT

Energy communities (ECs) are currently seen as an important pathway to increase the participation of citizens in the energy transition. The present work proposes a mixed integer linear programming (MILP) optimization model that provides the optimal design of a renewable energy community (REC) in terms of best technologies and chosen members. Different objective functions are investigated so that the REC's design can be studied from different perspectives. The first objective is related to the minimization of total annualized costs (TAC) while the second one regards the maximization of the shared energy. The model considers one year as time horizon with a timestep of one hour. A case study is defined by considering the municipality of Plodio, located in the northwest of Italy, as the host of a potential REC. A total of 11 possible users are introduced, including municipality and residential users. In cost-optimized scenarios, the REC design is characterized by fewer users but has the maximum installation of PV modules. However, most of the revenues are obtained due to the selling of electricity and not due to its sharing. When the shared energy is maximized, all the candidate members are chosen and technologies such as wind turbines and batteries are exploited to increase the number of periods characterized by the injection of electricity into the grid. It is also noted that higher electricity prices increase the profitability of the investment. Finally, it is shown that the inclusion of an industrial user positively influences energy-sharing indicators.

1. Introduction

Energy communities play a crucial role in the decentralization and decarbonization of electricity generation, empowering citizens, municipalities, and small business in the energy transition. By fostering local energy production and consumption, these communities not only reduce reliance on centralized power systems but also enhance energy security, create economic opportunities, and promote environmental sustainability as described in [1].

In 2019, the EU introduced the Clean Energy for All Europeans package to support the European Green Deal by promoting clean energy and setting decarbonization targets [2]. A key directive introduced by the package is the Renewable Energy Directive 2018/2001/EU (RED II), which aims for 32 % of the EU's energy to come from renewable sources by 2030 [3]. By 2020 the EU had achieved 22 % renewable energy [4], exceeding its previous target but still 10 % short of the 2030 goal. Alongside these targets, the RED II also introduces the concepts of Renewable Energy Communities (RECs) and collective self-consumers (CSCs), as described in [5]. CSCs are groups of at least two jointly acting renewables self-consumers within the same building or multi-apartment block, either sharing a single delivery point or having individual points for each consumer [6]. Conversely, RECs are legal entities where members, including individuals, small businesses, and local authorities, collaboratively produce and share renewable energy. The main goal of RECs is to provide environmental, economic, or social benefits rather than to make a profit [7]. Given the recent introduction of the REC concept, stakeholders still face challenges in planning energy communities, particularly when considering the techno-economic aspects of energy assets, the energy consumption behavior of each potential user, and the local regulatory framework. Therefore, it is imperative to develop tools that can support this decision-making process, and which can be applied to a realistic context of energy communities.

Different studies address the application of optimization models in energy communities planning and/or management, where the optimization process is carried out either by a commercial software or by a mathematical model written in a programming and numeric computing

* Corresponding author.
E-mail addresses: brulau@dtu.dk (B. Laurini), stefano.bracco@unige.it (S. Bracco).

https://doi.org/10.1016/j.segan.2024.101545
Received 23 January 2024; Received in revised form 26 August 2024; Accepted 2 September 2024
Available online 15 October 2024

Nomenclature

Sets

t	Time
u	User
m	Wind turbine model
r	Roof orientation

Parameters

A	Surface area
B	Equation of time coefficient
BEN	Benefit
C	Cost
CAPEX	Capital expenditure
CF	Capacity factor
CRF	Capital recovery factor
CO_2	CO_2 emissions
D	Demand
DCF	Discounted cash flow
DEL	Discounted electricity
DR	Discount rate
E	Energy
EOH	Equivalent operating hours
EQT	Equation of time
G	Irradiance
l	Lifetime
M	Big M (a large number)
LON	Longitude
LSM	Standard meridian longitude
n	Number of the day in a year
N	Number of installed technologies
OPEX	Operational expenditures
P	Produced power
Rb	Ratio of beam radiation on tilted surface
SOC	State of charge
T	Temperature
v	Speed

Greek letters

α	Altitude angle
β	Tilt
ε	Emission factor
ξ	Incentive
δ	Declination angle
θ	Incidence angle
θ_z	Zenith angle
γ	Azimuth angle
η	Efficiency
τ	Hour (local or solar)
ω	Hour angle
ϕ	Latitude
μ	Temperature coefficient
ψ	Power law exponent

Index

a	Air
b	Bought
beam	Beam radiation
BESS	Battery energy storage system
ch	Charging
cell	Cell related
DB	Dry-bulb
dch	Discharging
diff	Diffuse radiation
EC	Energy community
el	Electrical
grid	National grid
H	Horizontal
max	Maximum
min	Minimum
mod	Module
opt	Optimal design
PV	Photovoltaic module
rated	Rated
ref	Reference case
refl	Reflected radiation
RES	Renewable energy sources
s	Sold
shared	Shared quantity
sol	Solar
spl	Spline fitting
T	Tilted
user	User related
uni	Unitary
yearly	On annual basis
wind	Wind related
WT	Wind turbine

Decision variables

$D_{t,u}^{el,real}$	Real electrical demand of user *u* at time *t*
U_u^{user}	Binary variable related to each user participation in the REC
$P_{t,u}^{PV}$	AC PV power produced by prosumer *u* at time *t*
N_u^{PV}	N° of PV modules installed for user *u*
$CAPEX_u^{yearly}$	Annualized capital cost of user *u*
$OPEX_u^{yearly}$	O&M cost of user u
$P_{t,u,m}^{WT}$	Overall power produced by the *m* WT model of user *u* at time *t*
$P_{t,u}^{WT}$	Overall power produced by all the WTs models of user *u* at time *t*
$N_{u,m}^{WT}$	N° of *m* WT models installed for user *u*
$P_{t,u}^{BESS,ch}$	BESS charging power of user *u* at time *t*
$P_{t,u}^{BESS,dch}$	BESS discharging power of user *u* at time *t*
N_u^{BESS}	N° of installed BESS for user *u*
$x_{t,u}^{BESS,ch}$	Binary decision variable related to the BESS charging phase of user *u* at time *t*
$x_{t,u}^{BESS,dch}$	Binary decision variable related to the BESS discharging phase of user *u* at time *t*
$E_{t,u}^{BESS}$	BESS stored energy of user *u* at time *t*
$P_{t,u}^{grid,b}$	Power bought from the national grid by user *u* at time *t*
$P_{t,u}^{grid,s}$	Power sold to the national grid by user *u* at time *t*
$x_{t,u}^{grid,b}$	Binary decision variable related to the purchased power of user *u* at time *t*
$x_{t,u}^{grid,s}$	Binary decision variable related to sold power of user *u* at time *t*
$E_t^{shared,EC}$	Overall shared energy at time *t*
$E_t^{grid,b}$	Overall energy bought at time *t*
$E_t^{grid,s}$	Overall energy sold at time *t*
y_t^{shared}	Binary decision variable related to the sharing of energy at time *t*
$BEN_t^{shared,EC}$	Benefit obtained due to the sharing of energy at time *t*
$OPEX_{t,u}^{grid}$	Variable costs related to buying and selling energy from/to the grid for user of *u* at time *t*
$D_{t,u}^{el,real}$	Real electrical demand of user *u* at time *t*
U_u^{user}	Binary variable related to each user participation in the REC
$P_{t,u}^{PV}$	AC PV power produced by prosumer u at time *t*

environment, such as MATLAB or Python. As highlighted in [8], most of the studies propose models and tools mainly devoted to the assessment of RECs from the energy and financial point of view, whereas environmental and spatial criteria have a marginal role among both inputs and outputs. Moreover, as reported by [9], much still needs to be done to regulate the behaviour of storage systems within RECs. The studies reported in the literature can be further differentiated by the network that connects users within the community. Some of them propose a microgrid-based model where a private network is considered and the installation of physical links (i.e. cables) between users is a decision variable, i.e., an output of the optimization model. An example of such analysis is proposed in [10], where a model of a local energy community considering multi-energy flows and distributed generation technologies (DG) is presented. In this case, an optimal design is provided by the minimization of total costs, given by the sum of the costs for each site included in the model and possible electrical or thermal connections between them (e.g., electrical cables or heat pipes). A case study was performed considering the NTU campus in Singapore and its characteristics. Results showed that the connection of different sites through a district cooling network with distributed cold thermal energy storage is chosen for both purely economic and low-carbon scenarios. This is driven by a reduction in the peak cooling power capacity. Additionally, the tool chooses to install PV modules to meet the target reduction of primary energy imposed in low-carbon scenarios, and a high-efficiency trigeneration system when the primary energy reduction target is set to 20 %.

Another study addressed the impact of building and energy source characteristics under the economic, environmental and resilience point of view of a community [11]. More specifically, two baseline residential models, one natural gas based and one fully electrified, are compared with their cost-optimized and net-zero counterparts. The models are applied considering the location of Longmont, CO in the USA. Aiming at achieving resilience goals, the community's performance was accessed using the REopt Lite software developed by NREL, where the influence of outages can be studied. Overall, it is noted that there is a trade-off between initial costs and annualized costs when comparing baseline electrified and gas-based designs. For the optimized cases, electrified communities have higher capital costs and require more on-site generation than gas communities.

Focusing on the European scenario regarding energy communities, an optimal design model was developed in [12] considering the German regulatory framework. The research is based on a Mixed Integer Linear Programming (MILP) optimization model for assessing the implementation of multi-energy systems in an energy community formed by multi-family buildings (MFBs), also considering the legal differentiation between investor and user. The German Tenant Electricity Law (TEL) is applied to the model since it incentivizes landlords, which can act as the tenant's electricity contractor, to install PV or Combined Heat and Power (CHP) technologies in MFBs. In this case, landlords can profit from on-site consumption and other incentives, including subsidy payment per kWh, levy, and fee exceptions, where the incentive remuneration is dependent on the size of the installed technologies. The optimization model concerns the maximization of Net Present Value (NPV) reflecting the economic performance over 20 years. In order to enable the modelling of technologies with different lifetimes, reinvestment and residual costs are considered in the discounted cost of investment. The results indicate a bias towards CHP technologies within the framework studied, raising concerns about whether this could impact on current national CO_2 reduction targets. On the other hand, in [13] the authors propose an optimization model focused on the capacity sizing and flow management of RECs under the Italian regulatory framework, and different physical and virtual sharing schemes for centralized and decentralized configurations are compared.

Demand side management (DSM) can also provide positive results related to savings and the sharing of renewable energy inside a REC as shown in [14], where a linear optimization model that decides the optimal investment, considering the Italian scenario, is proposed. The distribution of the EC benefits is also analyzed by comparing different business models to the most optimal benefit distribution for each user. The study highlights the benefits of DSM and shows how the heterogeneity of the community composition affects savings and renewable energy consumption. Furthermore, in [15] the Italian EC regulatory framework is analyzed and a novel methodology for the design and management of energy community initiatives is proposed [15]. The optimization problem has been formulated as a two-stage MILP problem, involving investment decisions (first stage) and operation decisions (second stage). The objective function chosen was based on the minimization of the Total Annualized Costs (TAC) of the community model. Five typical days were used to represent different yearly periods/conditions. The main findings support electrification, demonstrating that a PV system combined with a heat pump can effectively reduce costs. Additionally, the methodology based on Shapley value for income distribution encourages users to shift their consumption towards periods of high PV generation.

In [16], a MILP optimization model was developed to provide optimal planning for a REC in Austria. The model introduces the possibility of transferring renewable energy between REC participants and considers node-specific electricity rates and market signals. Additionally, the model accounts for full-scale yearly optimization, covering 8760 hours. Overall, optimization results show a reduction in total energy costs by 15 % and CO_2 emissions by 34 %. On the other hand, in [17], an innovative methodology was presented to optimally design a multi-vector energy hub. This hub is capable of supplying electricity and thermal energy for space heating and cooling to a set of buildings within a sustainable district acting as a local energy community. A significant reduction in both CO_2 emissions and operational costs is achieved through the investment in a multi-energy system, when compared to the baseline scenario.

The integration of innovative technologies, such as renewable power plants, storage systems, and electric vehicles (EVs), is crucial not only in distributed generation facilities and microgrids [18], but also in the context of energy communities (ECs). Locally produced renewable energy can meet the increasing electricity demand for EV charging [19]. An example of this integration is investigated in [20], where a multi-energy system's optimal design and operation strategy is achieved through a MILP model, considering an eco-town in the UK. Among the results, smart charging of EVs allows for a cost reduction of around 12 % when compared to uncontrolled charging. Similarly, another MILP optimization model was developed in [21] to design optimal electric mobility services for a local energy community. This model was applied to the existing polygeneration microgrid of the Savona campus in Italy, with the potential to increase on-site generation capacity by adding more PV modules and storage technologies to meet transportation demand effectively.

A review of methodologies regarding the sizing and management of energy communities is presented in [22]. The studies are organized into different categories, including business models, electricity pricing and benefit distribution, energy system modelling, and objective function and optimization methods. Among the major trends, the review shows that most of the studies deal with PV and BESS in the community model, while fewer consider EVs and wind turbines. Also, economic goals dominate over the others, while non-economic goals that consider technical, environmental, and social aspects are being increasingly used. The model proposed in [23] computes the optimal capacity of each technology, namely solar PV and wind, as well as the optimal shared electricity among REC members in each time period. In [24] the authors investigate the impact of different energy community configurations on the distribution network and highlight the importance of designing a REC through a correct coupling between loads and generators for ensuring grid compliance. Similarly, in [25], the authors show that the strategic placement and sizing of PV and battery systems within Renewable Energy Communities (RECs), across different configurations such as city, suburban, and village grids, can significantly influence the performance and voltage profiles of distribution grids. As assessed in [26], sharing energy within RECs reduces energy losses in the grid, peak loads and reverse power flows and results in a smoother voltage profile. RECs can also play a challenging role within electricity markets [27], as discussed in [28] where it is proved that they can enhance the efficient use and stability of distribution grids by providing upward and downward flexibility services.

As stated in some of the previously mentioned studies, different configurations of ECs and the aggregation of their members can have a significant impact on community economics and local self-consumption of electricity. This is investigated in [29], where a tool based on multi-objective optimization and a Genetic Algorithm (GA) is developed to assist in the planning and operation of RECs. It focuses on finding the best combination of users and the allocation of solar energy within the community. Although not explicitly developing an optimal planning tool, the authors of [30] propose guidelines for the optimal economic aggregation of prosumers in ECs. More specifically, the study shows the importance of complementarity between the demand and generation of different prosumers for both CEC and REC configurations. Additionally, the study also addresses important features such as fair cost allocation among community members and demand-response programs. The work carried out in [31] offers an in-depth examination of various EC configurations, considering different community sizes, prosumer ratios, and installed PV capacities. It assesses their effects on critical performance indicators, including individual prosumer profitability, community self-sufficiency, and the implications for existing grid infrastructure. In [32], a multi-agent approach is adopted to model ECs, differentiating the actions and goals of community members from those of the centralized community energy manager. A member's decision is modeled in a stochastic manner according to their willingness to be flexible and follow the energy manager's recommendations. In turn, the latter aims to minimize the collective net energy exchanged with the grid. Different simulations are conducted to emulate scenarios with various community compositions in terms of member types. The authors in [33] present a multi-criteria optimization approach to enhance the design and operation of ECs by minimizing costs and greenhouse gas emissions. The study explores various EC configurations, including individual prosumers, CECs, RECs, and Hybrid Communities (HC). Moreover, it integrates two demand-side management strategies, the first focusing on adjustments to electricity demand based on price variations, and the second, presented as a novel approach, relying on adjusting the demand profile based on the availability of solar energy. Key performance indicators such as total cost of energy, specific GHG emissions, self-consumption rates, and grid usage are used to evaluate the effectiveness of these configurations and strategies. The study demonstrates that ECs generally outperform individual prosumers, with DSM strategies significantly reducing costs, emissions, and grid reliance.

From the literature review, it is evident that while significant progress has been made in the optimization of energy communities, some gaps remain unaddressed and other features are little explored. For example, many existing PV power models are based on input solar irradiance data that do not account for the orientation of PV modules (i.e., tilt and azimuth). However, energy communities often consist of buildings with roofs oriented in various directions, making it essential to include solar irradiance models that consider these orientations for accurate energy predictions. Moreover, few optimization models evaluate the positive or negative impact of individual users on the overall energy community. Understanding this impact is crucial for developing strategies to enhance the energy-sharing potential within the community.

This paper proposes a MILP model for the optimal design of a REC in terms of the best technologies to be installed and the best users to be selected as members of the community. Different objective functions are considered in order to investigate how the design of the REC can change as a function of the perspective adopted. The main contributions of this paper are:

- User selection optimization: Incorporating binary decision variables for user selection, allowing decision-makers to identify potential improvements within the community as a function of the chosen members.
- Detailed PV system modelling: Providing a detailed and validated model of PV systems where solar angles are estimated to forecast orientation-dependent power production on different roofs within the community.
- Study of a real scenario: Applying the model to a real candidate community represented by a small municipality within the Italian regulatory framework.

These attributes were chosen to be incorporated into the mathematical model described in the present paper, which is structured as follows. In Section 2 the transposition of the RED II into the Italian context is discussed. In Section 3 the mathematical model is described by characterizing the physical behaviour of the considered technologies and their costs, as well as the interaction of the possible REC users with the distribution grid. In Section 4 the case study is defined by analysing the application of the MILP model to a small Italian municipality. The results are presented and discussed considering different scenarios and applying a sensitivity analysis. Finally, conclusions about the research are drawn in Section 5 while also pointing out possible future improvements and development of the model.

2. Energy community framework in Italy

The Italian transposition of the RED II directive started in 2020, by the Law n.8/2020, introducing the definition of REC and jointly acting renewable self-consumers within the Italian legislation. In the case of RECs, the concept of physical proximity was translated by imposing that the participants of the energy community must be connected to the same secondary substation. This means that community participants had to be supplied by the same low-voltage distribution network. This differs for each EU member state, e.g., in Germany, at least 75 % of the voting rights in a REC must be held by natural persons residing in a postcode area that falls entirely or partially within a 50 km radius of the plant. On the other hand, on Spain, participants have to be located in a radius of 2000 m and be connected to the same low-voltage network [34]. Considering the Italian scenario again, a limit of installed capacity of the REC's power plants was established as 200 kW for each plant. Later, on 16th of September 2020, the *Ministero dello Sviluppo Economico* (MISE) implemented a ministerial decree that sets feed-in premium incentives for shared energy. Specifically, they were defined as 110 €/MWh for RECs and 100 €/MWh for CSC, applied to each kWh of shared energy over the relevant period. In the two cases, the incentive is valid for 20 years, and it is only applied for RES power plants built after the 1st of March 2020. Moreover, the *Autorità di Regolazione per Energia Reti e Ambiente* (ARERA), by the resolution 318/2020/R/eel, established the return of grid tariffs due to savings in transmission and distribution of electricity. These components account for 7.78 €/MWh and 0.59 €/MWh due to saving transmission and distribution of electricity, respectively. In the case of CSC, there is also a benefit associated with the avoided grid losses, which is dependent on the voltage level and on the *Prezzo Zonale Orario* (i.e., Zonal hourly price) of electricity. Together with the feed-in premium incentive these returns components are determined according to the shared energy inside the REC or CSC scheme, which is calculated for every hour as the minimum between the sum of the energy injected into the grid and the sum of the energy absorbed from it by the final users. The new legislative decree 199/21 introduced some modifications regarding the REC's size. The maximum limit of each RES plant was changed from 200 kW to 1 MW and the RECs perimeter was enlarged by allowing the participation of users that are connected to the same primary substation. This enables the creation of larger RECs, both in terms of perimeter and installed capacity. The overall benefit associated with the shared energy inside a REC or CSC is due to the feed-in premium incentive (i.e., at the time this study was developed, equal to 110 €/MWh or 100 €/MWh) and to the returns of grid tariffs. Moreover, it is also possible to request to the *Gestore dei Servizi Energetici* (GSE) the withdrawal of the energy fed into the grid by the community's plants, at the market energy price [35]. The feed-in premium incentive has recently been revised and in November 2023 the EU Commission approved the new regulation drawn up by the Italian Ministry for the Environment and Energy Security. The full implementation of RED II took place with the Legislative Decree no. 199 of 8 November 2021 and the following acts. In particular, the Decree of the Minister of Environment and Energy Security of 7 December 2023, no. 414 (CACER Decree), in force since 24 January 2024, defines the new modalities for the granting of incentives aimed at promoting the installation of plants powered by renewable sources included in configurations of energy communities, groups of self-consumers and remote self-consumers. Moreover, the "Testo Integrato per l′Autoconsumo Diffuso" (TIAD), annexed to ARERA Resolution 727/2022/R/eel, regulates the operating mechanism and the valorisation contributions due to the energy consumed within the authorised configurations. As previously introduced, the maximum size of the plant eligible to be included within a REC has been increased to 1 MW and the scope of the community has been extended to include all users connected to the same primary high-voltage/medium-voltage substation.

3. Mathematical model

The proposed MILP optimization model uses a set of input data and parameters to provide a first optimal configuration of the REC based on the minimization of costs and a second one based on the maximization of the shared energy. Some of the inputs are geographical and weather information about the considered site, capital and operational costs of technologies, energy and incentive prices, and electrical demand profiles. The model was developed in MATLAB using YALMIP toolbox [36], which is a relevant tool for optimization problems. The optimization process was carried out by the GUROBI solver [37].

As mentioned before, the mathematical model includes some innovative aspects regarding optimal REC planning. First, the temporal resolution of the model can be considered high for planning problems since the time horizon is 8760 hours, with a timestep of 1 hour. Second, the PV power is estimated as a function of the tilt and azimuth angles of each user's roof. The model enables the inclusion of two different orientations in the same roof, which is a quite common attribute of residential buildings. Additionally, the model can provide the optimal selection of REC members, considering the specific objective function, which in this case is either described by total annualized costs or overall energy shared inside the community.

3.1. Input data preprocessing and curation

The preprocessing and data curation procedures in this subsection are implemented before the formal definition of the MILP problem. These include the generation of synthetic load profiles and the modelling of energy production from single renewable generators.

3.1.1. Load profiles

One of the inputs of the optimization model is represented by the load profiles of the users. In Italy, as in many other countries, only a few domestic and public sector users have meters capable of providing hourly or quarter-hourly consumption values. In the majority of cases, the only information available to estimate daily load profiles is represented by monthly consumption data and the committed power value. It is therefore necessary to use reference load profiles available from databases or reports produced by research organisations or private companies. The selection of the reference load profiles typically considers similar users located in areas belonging to the same climate zone as the examined case. Moreover, it is important to highlight that, in Italy, the electricity bill is usually broken down into a number of different cost components. The component related to energy consumption may be calculated according to three time-dependent bands: F1, F2 and F3. They are classified as follows [38]:

- F1 band: from Monday to Friday, from 8:00–19:00, excluding national holidays.
- F2 band: from Monday to Friday, from 7:00–8:00 and from 19:00–23:00, excluding national holidays; on Saturdays from 7:00–23:00, excluding national holidays.
- F3 band: from Monday to Saturday, from 00:00–7:00 and from 23:00–24:00; on Sundays and holidays, all hours of the day.

By collecting monthly and yearly demand data from electricity bills of users, overall consumption values on each band can be obtained, i.e., $E^{F1,tot}$, $E^{F2,tot}$ and $E^{F3,tot}$. The load profiles were generated by scaling reference load profiles according to these known consumption values. A similar approach is used in HOMER's load profiles generator, where a reference load profile is scaled to generate a new one [39]. Nevertheless, in this case three different scaling factors are used instead of one, since there are three different electricity bands. Using three scaling factors allows the scaling process to better capture the different temporal behavior of energy consumption.

3.1.2. Model of a single PV module

In order to estimate the incident irradiance on the PV module's surface, solar angles need to be defined. The computation of such angles allows the model to estimate the position of the sun in the sky at each time *t*. Hence, by using input data such as geographic information about the PV plant site, the azimuth of the surface (γ_u^{PV}) and its tilt (β_u^{PV}), it is possible to calculate the global irradiance on the tilted PV surface ($G_{t,u}^T$) for user *u* at time *t* [40,41]. Note that the model of a single PV module described in this subsection does not involve any decision variables, hence, being developed as a combination of different input parameters of the model.

Computations related to solar angles are given by Eqs. (1)–(8):

$$\delta_t = 23.45 \cdot \pi \Big/ 180 \cdot \sin\left(2\pi \cdot \frac{284+n}{365}\right) \quad t = 1, \ldots, T \tag{1}$$

$$B_t = (n-81) \cdot \frac{360}{364} \quad t = 1, \ldots, T \tag{2}$$

$$EQT_t = 9.87 \cdot \sin(2B_t) - 7.53 \cdot \cos(B_t) - 1.5 \cdot \sin(B_t) \quad t = 1, \ldots, T \tag{3}$$

$$\tau_t^{sol} = \tau_t^{loc} + \frac{EQT_t}{60} + \frac{LON - LSM}{15} \quad t = 1, \ldots, T \tag{4}$$

$$\omega_t = (\tau_t^{sol} - 12) \cdot 15 \quad t = 1, \ldots, T \tag{5}$$

$$\alpha_t^{sol} = \arcsin(\cos(\varphi) \cdot \cos(\delta_t) \cdot \cos(\omega_t) + \sin(\varphi) \cdot \sin(\omega_t)) \quad t = 1, \ldots, T \tag{6}$$

$$\theta z_t = 90 - \alpha_t^{sol} \quad t = 1, \ldots, T \tag{7}$$

$$\gamma_t^{sol} = sign(\omega_t) \cdot \arccos\left(\frac{\cos(\theta z_t) \cdot \sin(\varphi) - \sin(\delta_t)}{\sin(\theta z_t) \cdot \cos(\varphi)}\right) \quad t = 1, \ldots, T \tag{8}$$

where δ_t is the declination angle, n is the number of the day over the year, B_t is a day-dependent parameter, EQT_t is the equation of time (given in minutes), τ_t^{sol} is the solar time, τ_t^{loc} is the local time, LON is the site's longitude, LSM is the time zone's standard meridian, ω_t is the hour angle, α_t^{sol} is the solar altitude angle, φ is the site's latitude, θz_t is the zenith angle and γ_t^{sol} is the solar azimuth angle.

The solar incidence angle ($\theta_{t,u,r}$) is the angle between the sun's rays and the tilted surface, i.e., the PV module. It considers the module's tilt and azimuth, which are user-dependent input parameters. Moreover, it can also consider roofs that have different R orientations, for the same user u.

$$\theta_{t,u,r} = \arccos\left(\cos(\theta z_t)\cdot\cos\left(\beta^{PV}_{u,r}\right) + \sin(\theta z_t)\cdot\sin\left(\beta^{PV}_{u,r}\right)\cdot\cos\left(\gamma^{PV}_{u,r} - \gamma^{s}_{t}\right)\right)$$
$$t = 1,\ldots,T \quad u = 1,\ldots,U \quad r = 1,\ldots,R \tag{9}$$

The ratio of beam radiation on tilted surface ($Rb_{t,u,r}$) can be used to determine the overall irradiance that arrives on the tilted PV surface using horizontal irradiance values as input:

$$Rb_{t,u,r} = \frac{\cos(\theta_{t,u,r})}{\cos(\theta z_t)} \quad t = 1,\ldots,T \quad u = 1,\ldots,U \quad r = 1,\ldots,R \tag{10}$$

Finally, the global irradiance ($G^{T}_{t,u,r}$) that arrives on the tilted PV surface is a function of three components, the beam ($G^{T,beam}_{t,u,r}$), the diffuse ($G^{T,diff}_{t,u,r}$) and the reflected one ($G^{T,refl}_{t,u,r}$):

$$G^{T}_{t,u,r} = G^{T,beam}_{t,u,r} + G^{T,diff}_{t,u,r} + G^{T,refl}_{t,u,r} \quad t = 1,\ldots,T \quad u = 1,\ldots,U \quad r = 1,\ldots,R \tag{11}$$

$$G^{T}_{t,u,r} = G^{H}_{t}\cdot\left(1 - \frac{G^{H,diff}_{t}}{G^{H}_{t}}\right)\cdot Rb_{t,u,r} + G^{H,diff}_{t}\left(\frac{1+\cos\left(\beta^{PV}_{u,r}\right)}{2}\right) + G^{H}_{t}\cdot\rho\cdot\left(\frac{1-\cos\left(\beta^{PV}_{u,r}\right)}{2}\right) \quad t = 1,\ldots,T \quad u = 1,\ldots,U \quad r = 1,\ldots,R \tag{12}$$

where G^{H}_{t} and $G^{H,diff}_{t}$ are the global irradiance on a horizontal surface and the diffuse irradiance on a horizontal surface, respectively. These values are acquired on a yearly basis using the Photovoltaic Geographical Information System (PVGIS) tool [42]. Also, ρ represents the average reflectivity of the nearby surfaces (i.e., the albedo).

By knowing the global irradiance incident on the PV module's surface, it is possible to estimate the PV power produced by the module ($P^{PV,uni}_{t,u,r}$):

$$P^{PV,uni}_{t,u,r} = \left\{\eta^{PV,ref}\cdot\left[1 - \mu\cdot\left(T^{cell}_{t,u,r} - T^{cell,STC}\right)\right]\right\}\cdot G^{T}_{t,u,r}\cdot A^{PV}$$
$$t = 1,\ldots,T \quad u = 1,\ldots,U \quad r = 1,\ldots,R \tag{13}$$

where $\eta^{PV,ref}$ is the module's efficiency at Standard Test Conditions (STC), μ is the temperature coefficient, $T^{cell,STC}$ is the temperature of the PV cell at STC and A^{PV} is the module's surface area. The term inside brackets regards the PV module's efficiency correction due to temperature variation, which considers the actual temperature of the cell ($T^{cell}_{t,u,r}$) [43]. The cell temperature can be calculated as:

$$T^{cell}_{t,u,r} = T^{a,DB}_{t} + \left(T^{cell,NOCT} - 20\right)\cdot\frac{G^{T}_{t,u,r}}{800}$$
$$t = 1,\ldots,T \quad u = 1,\ldots,U \quad r = 1,\ldots,R \tag{14}$$

where $T^{cell,NOCT}$ is the temperature of the cell at Nominal Operating Condition (NOCT), which can also be found on the datasheet of the module.

$N^{PV,\max}_{u,r}$ is the maximum number of modules that can be installed for user u, given a specific roof orientation r. This value is a function of the module's area ($A^{PV,\mathrm{mod}}_{u}$) and the area available for installing PV modules ($A^{PV,\max}_{u,r}$), which are input parameters of the MILP model:

$$N^{PV,\max}_{u} = floor\left(\frac{A^{PV,\max}_{u,r}}{A^{PV,\mathrm{mod}}_{u}}\right) \quad u = 1,\ldots,U \quad r = 1,\ldots,R \tag{15}$$

3.1.3. PV module's model validation

Since photovoltaic systems are being considered as the backbone of renewable energy communities, careful attention was given to this technology in the present model. A validation step was conducted based on NREL's PV module performance validation database [44,45], to verify if the developed PV model was sufficiently accurate. First, weather and geographical information were used as input parameters to estimate the module's power production, by using (13). Then, the power production was compared to the real power measured in the NREL's experiment represented in the "NREL_Cocoa_HIT05667" file, considering a period of approximately one month of operation.

Fig. 1 shows the comparison between real measured data and the estimated ones. It is noted that there is a small difference between the estimated cell temperature, calculated by (14), and the measured one, but this difference does not imply a considerable difference in PV power estimation. On the contrary, it is possible to see that both the estimated solar irradiance and PV power accurately match their real measured counterparts. In particular, the mean error and the mean relative error associated with the power forecasting are 4.63 W and 7.48 %, respectively.

3.1.4. Model of a single wind turbine

The wind turbines considered as possible technologies in the REC were modelled by estimating their production through power curves. This estimation was performed using datasets of power output and wind speed, provided in the datasheet of the different wind turbine models. The power curve of a wind turbine can be described by 4 main regions, as shown in Fig. 2 [46]. When the speed of the wind (v^{wind}) is lower than the cut-in speed (v^{cut-in}) no power is produced since the wind's kinetic energy is too low to turn the turbine's rotor. Between the cut-in and the rated speed ($v^{WT,rated}$) the power produced varies in a non-linear way. After the turbine reaches its rated speed, it can maintain its nominal power until the wind speed reaches the cut-out speed ($v^{cut-out}$), then the turbine rotor is halted to prevent damage to the turbine and its system components.

Together with the discrete power curve data set, datasheets also provide: v^{cut-in}, $v^{WT,rated}$, $v^{cut-out}$. Therefore, the power production at regions 1, 3 and 4 are known according to these values. Region 2 can be estimated by fitting a polynomial or spline to the discrete dataset values of wind power and wind speed [47]. In this model, a spline fitting was used, and the power produced by the wind turbine model m at time t for user u ($P^{WT,uni}_{t,u,m}$) was estimated considering the following equations:

$$P^{WT,uni}_{t,u,m} = \begin{cases} 0, & v^{wind}_{t,u} < v^{cut-in}_{m} \text{ or } v^{wind}_{t,u} > v^{cut-out}_{m} \\ P^{WT,spl}_{m}, & v^{cut-in}_{m} \leq v^{wind}_{t,u} < v^{WT,rated}_{m} \\ P^{WT,rated}_{m}, & v^{WT,rated}_{m} \leq v^{wind}_{t,u} \leq v^{cut-out}_{m} \end{cases} \tag{16}$$
$$t = 1,\ldots,T \quad u = 1,\ldots,T \quad m = 1,\ldots,m$$

where $v^{wind}_{t,u}$ was assessed using the database provided by the "*Ricerca Sistema Energetico*" (RSE) Wind Atlas [48]. The database is composed of windspeed measurements at 5 different heights: 50 m, 75 m, 100 m, 125 m and 150 m.

The wind vertical speed profile is defined by a boundary layer that forms on the earth's surface, where mean wind speeds are generally lower than those observed at higher altitudes. The power law represents a simple model to describe this behavior [49]. Indeed, it can be used to estimate wind speeds at different heights by knowing the wind speed at a specific height and the power law exponent (ψ):

$$v^{wind,2} = v^{wind,1}\cdot\left(\frac{h_{ref,2}}{h_{ref,1}}\right)^{\psi} \tag{17}$$

The power law coefficient depends on many conditions, but it is mainly related to the terrain and its surface roughness. By having two different wind speed measurements at two different heights, for example, obtained from anemometers, it is possible to calculate ψ by

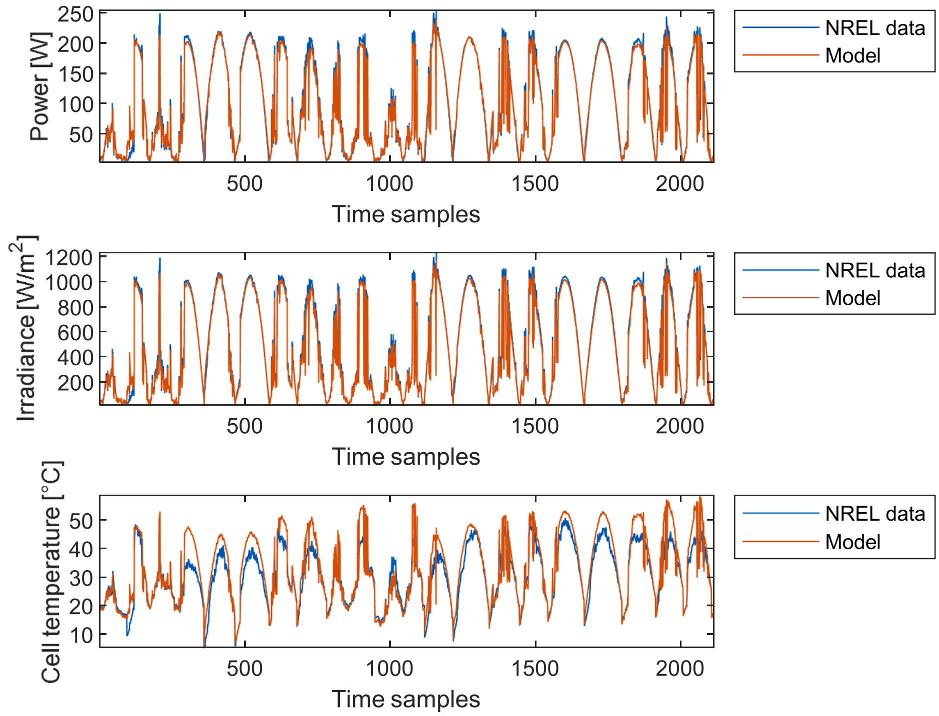

Fig. 1. PV model validation.

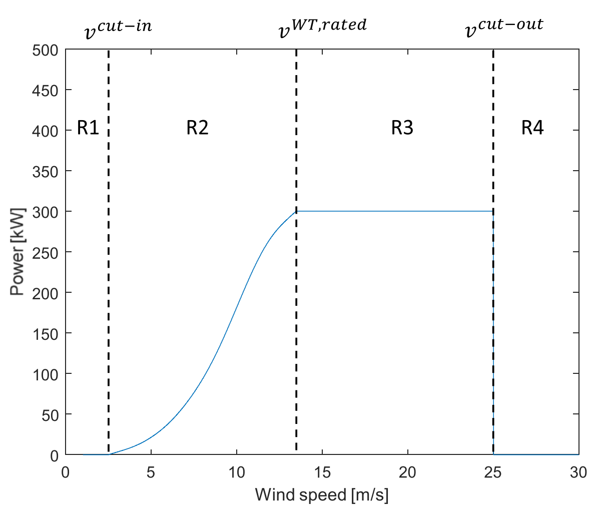

Fig. 2. Wind turbine power curve regions.

rearranging (17):

$$\psi = \frac{\log\left(\frac{v^{wind,2}}{v^{wind,1}}\right)}{\log\left(\frac{h^{ref,2}}{h^{ref,1}}\right)} \tag{18}$$

Finally, (15) is used to estimate the power production of each turbine model m.

3.2. Optimization problem definition

Here, the actual constraints and objective functions that define the MILP model are presented. Some of these constraints, such as those related to the renewable power plants, are developed based on the data preprocessing and curation described in the previous subsection.

3.2.1. User participation

A binary variable (U_u^{user}) is introduced to state whether a user is chosen to participate in the REC. The implementation of all technologies should be constrained by the user participation variable. It derives that the real electrical load profile of each user, candidate to be a member of the community, can be defined using the binary variable:

$$D_{t,u}^{el,real} = D_{t,u}^{el} \cdot U_u^{user} \quad t = 1, \ldots, T \quad u = 1, \ldots, U \tag{19}$$

where $D_{t,u}^{el}$ is the input electrical demand for each user, which is considered by the model only when the user is chosen as a member of the community (i.e. $U_u^{user} = 1$).

Moreover, according to the Italian REC regulation, the number of participants of the community must be higher than two. Such a constraint can be easily modelled as follows:

$$\sum_{u=1}^{U} U_u^{user} \geq 2 \tag{20}$$

3.2.2. PV plant model

The constraints that should be applied in the MILP model for the PV plants are:

$$0 \leq N_{u,r}^{PV} \leq N_{u,r}^{PV,\max} \cdot U_u^{user} \quad u = 1, \ldots, U \quad r = 1, \ldots, R \tag{21}$$

$$P_{t,u}^{PV} = \sum_{r=1}^{R} P_{t,u,r}^{PV,uni} \cdot \eta_u^{BOS} \cdot N_{u,r}^{PV} \quad t = 1, \ldots, T \quad u = 1, \ldots, U \tag{22}$$

where η_u^{BOS} is the Balance of the System (BOS) efficiency, which accounts for losses in the PV plant, such as DC-AC conversion inefficiencies, mismatching, shading, etc.

The annualized capital cost and O&M costs related to PV and the other technologies described in the section are defined in (23) and (24).

$$CAPEX_u^{yearly} = CRF_u \cdot CAPEX_u \cdot N_u \cdot P_u^{rated} \quad u = 1, \ldots, U \tag{23}$$

$$OPEX_u^{yearly} = OPEX_u \cdot N_u \cdot P_u^{rated} \quad u = 1, \ldots, U \tag{24}$$

where CRF_u is the capital recovery factor related to the technology. In general, the CRF allows the conversion of a fixed present value into an annualized equivalent series of discounted cash flows to be paid until the end of the technology's lifetime.

$$CRF = \frac{DR\cdot(1+DR)^l}{(1+DR)^l - 1} \tag{25}$$

(25) represents the method of calculating CRF for a generic technology, considering its lifetime (l) and a specific discount rate (DR).

3.2.3. Wind power plant model

Constraints were applied in the MILP model to limit the number of installed turbines for each user u:

$$N_{u,m}^{WT} \geq 0 \quad u = 1, \ldots, U \quad m = 1, \ldots, M \tag{26}$$

$$\sum_{m=1}^{M} N_{u,m}^{WT} \leq N_u^{WT,\max}\cdot U_u^{user} \quad u = 1, \ldots, U \tag{27}$$

where $N_u^{WT,\max}$ is the maximum number of wind turbines that can be installed for user u.

The overall wind power produced by each user is calculated as follows:

$$P_{t,u}^{WT} = \sum_{m=1}^{M} P_{t,u,m}^{WT,uni}\cdot N_{u,m}^{WT}$$

$$t = 1, \ldots, T \quad u = 1, \ldots, U \tag{28}$$

3.2.4. BESS model

Battery Energy Storage Systems (BESS) are usually proposed as possible components of microgrids [50] but they are often adopted in a REC to increase flexibility, reduce energy bills of the members and increase the shared energy in the community.

The dynamic equation that characterizes the energy that is stored in the BESS is a discrete transient energy balance, as shown in (29) where Δt indicates the duration of the time interval in the MILP model.

$$E_{t+1,u}^{BESS} = E_{t,u}^{BESS} + \left(P_{t,u}^{BESS,ch}\eta_u^{BESS,ch} - \frac{P_{t,u}^{BESS,dch}}{\eta_u^{BESS,dch}}\right)\Delta t \qquad t = 1, \ldots, T-1 \quad u = 1, \ldots, U \tag{29}$$

where $E_{t,u}^{BESS}$ is the amount of energy stored at time t by user u, $P_{t,u}^{BESS,ch}$ is the power used to charge the BESS, $\eta_u^{BESS,ch}$ is its charging efficiency, $P_{t,u}^{BESS,dch}$ is the power discharged from the BESS and $\eta_u^{BESS,dch}$ is its discharging efficiency.

Eq. (29) does not constrain the energy stored at the first timestep, i.e., $E_{1,u}^{BESS}$. Hence, an additional set of constraints needs to be introduced:

$$E_{1,u}^{BESS} = \left(\frac{SOC^{\min}}{100}\right)\cdot N_u^{BESS}\cdot E_u^{BESS.\max} \quad u = 1, \ldots, U \tag{30}$$

where $SOC^{\min}$ is the minimum state of charge and $E_u^{BESS.\max}$ is the maximum energy, in kWh, that can be stored in one battery.

Moreover, a minimum state of charge is also imposed for the other timesteps:

$$\left(\frac{SOC^{\min}}{100}\right)\cdot N_u^{BESS}\cdot E_u^{BESS.\max} \leq E_{t,u}^{BESS} \leq N_u^{BESS}\cdot E_u^{BESS.\max} \qquad t = 2, \ldots, T \quad u = 1, \ldots, U \tag{31}$$

The constraint (32) is adopted to avoid the simultaneous charge and discharge of the storage, where $x_{t,u}^{BESS,ch}$ is a binary variable that takes unitary value during charging phase and zero value during discharging phase or when the system is not working. Similarly, $x_{t,u}^{BESS,dch}$ is also a binary variable that takes unitary value during the discharging phase and zero value during the charging phase or in idle mode.

$$x_{t,u}^{BESS,ch} + x_{t,u}^{BESS,dch} \leq 1 \quad t = 1, \ldots, T \quad u = 1, \ldots, U \tag{32}$$

In order to limit the charging and discharging power of the BESS system installed for user u, the constraints (33–36) need to be introduced. The rationale is that these constraints can avoid the non-linearity which would be introduced by multiplying two decision variables, i.e., $x_{t,u}^{BESS,ch}$ (or $x_{t,u}^{BESS,dch}$) and N_u^{BESS}. Moreover, constraints (37) are introduced to avoid the possibility of charging the BESS using the external grid.

$$0 \leq P_{t,u}^{BESS,ch} \leq P_u^{BESS,ch,\max}\cdot N_u^{BESS} \quad t = 1, \ldots, T \quad u = 1, \ldots, U \tag{33}$$

$$P_{t,u}^{BESS,ch} \leq P_u^{BESS,ch,\max}\cdot N_u^{BESS,\max}\cdot x_{t,u}^{BESS,ch} \qquad t = 1, \ldots, T \quad u = 1, \ldots, U \tag{34}$$

$$0 \leq P_{t,u}^{BESS,dch} \leq P_u^{BESS,dch,\max}\cdot N_u^{BESS} \qquad t = 1, \ldots, T \quad u = 1, \ldots, U \tag{35}$$

$$P_{t,u}^{BESS,dch} \leq P_u^{BESS,dch,\max}\cdot N_u^{BESS,\max}\cdot x_{t,u}^{BESS,dch} \qquad t = 1, \ldots, T \quad u = 1, \ldots, U \tag{36}$$

$$x_{t,u}^{grid,b} + x_{t,u}^{BESS,ch} \leq 1 \qquad t = 1, \ldots, T \quad u = 1, \ldots, U \tag{37}$$

The installation limit of BESS is imposed in the same way as for PV and WT systems:

$$0 \leq N_u^{BESS} \leq N_u^{BESS,\max}\cdot U_u^{user} \tag{38}$$

Furthermore, it is assumed that BESS can only be installed for those users who have also a PV plant installed, as indicated in the constraint bellow:

$$N_u^{BESS} - N_u^{PV,\mathrm{mod}}\cdot M \leq \quad 0 \tag{39}$$

Where, according to the "Big M method" M, is a large number used to constrain N_u^{BESS} depending on the value of $N_u^{PV,\mathrm{mod}}$.

3.2.5. Interaction with the distribution grid

All participants of the REC are connected to the distribution grid by their electrical PODs. They can either absorb power from the grid ($P_{t,u}^{grid,b}$) or inject power into the grid ($P_{t,u}^{grid,s}$). Nonetheless, as in the BESS model, constraints (40)-(42) need to be introduced to avoid the simultaneous injection and absorption of power into/from the grid.

$$x_{t,u}^{grid,b} + x_{t,u}^{grid,s} \leq U_u^{user} \quad t = 1, \ldots, T \quad u = 1, \ldots, U \tag{40}$$

$$P_{t,u}^{grid,b} - x_{t,u}^{grid,b}\cdot M \leq 0 \quad t = 1, \ldots, T \quad u = 1, \ldots, U \tag{41}$$

$$P_{t,u}^{grid,s} - x_{t,u}^{grid,s}\cdot M \leq 0 \quad t = 1, \ldots, T \quad u = 1, \ldots, U \tag{42}$$

The CO_2 emissions embedded in the power absorbed from the grid can be calculated using the grid emission factor ($\varepsilon^{CO2,grid}$) of the specific country.

$$CO2_{t,u}^{grid} = \varepsilon^{CO2,grid}\cdot P_{t,u}^{grid,b}\cdot\Delta t \quad t = 1, \ldots, T \quad u = 1, \ldots, U \tag{43}$$

The variable costs related to buying or selling power from/to the grid are calculated as follows:

$$OPEX_{t,u}^{grid} = p_{t,u}^{el,b}\cdot\left(P_{t,u}^{grid,b}\cdot\Delta t\right) - p_{t,u}^{el,s}\cdot\left(P_{t,u}^{grid,s}\cdot\Delta t\right) \qquad t = 1, \ldots, T \quad u = 1, \ldots, U \tag{44}$$

3.2.6. Shared energy

At any time t, the active power balance must be respected for each user u.

$$P^{PV}_{t,u} + P^{WT}_{t,u} + P^{BESS,dch}_{t,u} + P^{grid,b}_{t,u} = D^{el,real}_{t,u} + P^{BESS,ch}_{t,u} + P^{grid,s}_{t,u} \quad t = 1,\ldots,T \quad u = 1,\ldots,U \tag{45}$$

As mentioned in Section 2, the Italian REC regulatory framework introduces an incentive applied to the energy that is shared inside the energy community, which is calculated for every hour as the minimum between the energy injected into the grid ($E^{grid,b}_t$) and the energy absorbed from it by all the members ($E^{grid,s}_t$):

$$E^{shared,EC}_t = \min(E^{grid,b}_t, E^{grid,s}_t) \quad t = 1,\ldots,T \tag{46}$$

However, the implementation of (46) would introduce a non-linearity to the model. To overcome this problem, the set of constraints from (47) to (52) can be defined to emulate the “min” function in a MILP context:

$$E^{shared,EC}_t \le E^{grid,b}_t \quad t = 1,\ldots,T \tag{47}$$

$$E^{shared,EC}_t \le E^{grid,s}_t \quad t = 1,\ldots,T \tag{48}$$

$$E^{shared,EC}_t \ge E^{grid,s}_t - M \cdot y^{shared}_t \quad t = 1,\ldots,T \tag{49}$$

$$E^{shared,EC}_t \ge E^{grid,b}_t - M \cdot \left(1 - y^{shared}_t\right) \quad t = 1,\ldots,T \tag{50}$$

$$E^{grid,s}_t \le E^{grid,b}_t + M \cdot y^{shared}_t \quad t = 1,\ldots,T \tag{51}$$

$$E^{grid,b}_t \le E^{grid,s}_t + M \cdot \left(1 - y^{shared}_t\right) \quad t = 1,\ldots,T \tag{52}$$

where y^{shared}_t is a binary decision variable used to enforce the definition of shared energy. It is 1 when $E^{grid,b}_t$ is higher than $E^{grid,s}_t$ and zero otherwise.

The overall benefit obtained due to the sharing of energy ($BEN^{shared,EC}_t$) inside the REC can be calculated as following:

$$BEN^{shared,EC}_t = E^{shared,EC}_t \cdot \left(\xi^{inc} + \xi^{ret}\right) \quad t = 1,\ldots,T \tag{53}$$

where ξ^{inc} indicates the explicit incentive associated with the shared energy, and ξ^{ret} is the return of grid-tariffs, due to saving in transmission and distribution of electricity.

3.2.7. Objective function

The MILP cost-related objective function regards the minimization of Total Annualized Costs (TAC). It is based on 4 cost components: the annualized capital costs expended by each user u ($CAPEX^{yearly}_u$), the annual operational costs expended by each user u ($OPEX^{yearly}_u$), the net operational expenditures related to buying and selling energy to the grid ($OPEX^{grid}_{t,u}$) and the overall hourly benefit obtained due to the sharing of energy inside the REC ($BEN^{shared,EC}_t$).

$$\min TAC = \min\left(\sum_{u=1}^{U} CAPEX^{yearly}_u + \sum_{u=1}^{U} OPEX^{yearly}_u + \sum_{u=1}^{U} \times \sum_{t=1}^{T} OPEX^{grid}_{t,u} - \sum_{t=1}^{T} BEN^{shared,EC}_t\right) \tag{54}$$

The second objective function considered regards the maximization of the shared energy inside the REC:

$$\max \text{Esh} = \min\left(-\sum_{t=1}^{T} E^{shared,EC}_t\right) \tag{55}$$

After the optimization, the savings with respect to the baseline case can be computed:

$$Savings = \frac{C_{base} - \left(OPEX^{total} - BEN^{shared,EC,total}\right)}{C_{base}} \cdot 100 \tag{56}$$

where C_{base} are the annual operational expenses in the baseline case, which are computed by the sum of the users bills when they do not form a REC. $OPEX^{total}$ and $BEN^{shared,EC,total}$ are the total annual operational expenses and the total annual benefits earned when the selected users form the REC proposed by the optimization model.

4. Results and discussion

The optimization model described in the previous section is general and it can be applied to any energy community model if updates regarding incentives and installation constraints are made. In this research, a case study was carried out considering the application of the model to the municipality of Plodio, Italy, which can be a potential candidate for hosting a REC.

4.1. Case study description

Plodio is a small municipality of the Savona province located in the Ligurian region in the northwest of Italy. It covers a land area of approximately 8.65 km^2 and hosts a total of 626 inhabitants, resulting in a populational density of 72.37 inhab/km^2 [51]. The installation of RES plants, such as PV systems, on buildings owned by the municipality has emerged as a potential approach for implementing renewable energy communities in Italy, leveraging the larger investment and organizational resources, as well as greater surface availability, of public entities. Therefore, special attention was given to the buildings in Plodio that are owned by the municipality.

Three main typologies of users were defined for the case study:

- Municipality (M): users whose buildings are owned by the municipality.
- Residential (R): residential users who, for some reason, are not able to install any renewable technology.
- Residential PV (RPV): residential users who can install PV modules on the roof of their buildings.

These kind of users represent an example of typical membership inside an EC, where municipality and some residential buildings are available to install PV modules on their roofs and other residential buildings are not. Fig. 3 presents the potential participants of the REC. There are a total of 4 municipality buildings, 5 conventional residential buildings and 2 residential buildings which can install PV modules on their roofs. The potential users are relatively scattered around the municipality, involving 3 main localities, from right to left on the map: *Piani*, *Fagioli* and *Chiesa*.

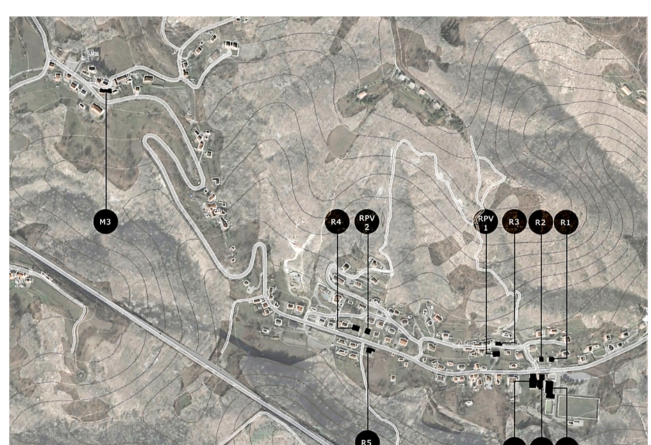

Fig. 3. Potential members of Plodio’s REC.

4.1.1. Case study input data

End-use load profiles for the U.S. building stock were used as a reference to generate demand profiles for each user [52], due to the lack of historical load profiles for buildings in Italy, given the recent introduction of smart meters. Then, yearly energy consumption in the three different electricity bands, available in electricity bills, was employed to scale these reference profiles. The municipality users had their yearly profiles estimated using real data from their electricity bills, while residential users had their yearly profiles estimated using real data from similar buildings located in the Liguria region. Table 1 shows the input data used for generating users' load profiles.

Similarly, Table 2 shows the user-related input data applied to the model. Note that some users have two azimuth orientations since their roofs are divided into two sections with opposite orientations. Conventional residential users (i.e., R1, R2, R3, R4, and R5) are not defined by such inputs as they are modelled as not eligible for PV plant installation. Moreover, the latitude and longitude values considered for the solar irradiance model were 44.35° and 8.26°, respectively.

The municipality's medical center (M4) already has a PV system with 8 kW peak capacity installed over a car parking canopy. Thus, this plant was included in the model by setting its CAPEX to zero, given that its installation was not an outcome of the optimization model itself.

The types of technologies included in the case study are a 400 W peak power monocrystalline PV module, a 7.2 kWh capacity BESS and 3 different medium-sized wind turbine models with rated power of 300 kW, 500 kW and 810 kW, respectively. Unitary technologies such as one wind turbine, PV module and BESS can be stacked by the optimization model to generate systems with larger sizes (e.g., an array of many PV modules), always respecting the installation constraints previously imposed. It is planned to install wind turbines on top of the hills facing the municipality.

Costs and lifetimes are assumed to estimate the annualized CAPEX of each technology. In particular, the PV's lifetime, CAPEX and annual OPEX are defined as 25 years, 2000 €/kW and 15 €/kW, respectively. For wind turbines, lifetime is also defined as 25 years, and capital costs vary according to their capacity, reaching a maximum of 3500 €/kW and a minimum of 3300 €/kW. Also, their annual OPEX is set to 100 €/kW independently of their size. Finally, BESS is characterized by a lifetime of 15 years, CAPEX of 700 €/kWh and annual OPEX of 20 €/kWh. It is important to mention that capital and operational costs are selected to be higher than those presented in recent reports about the cost of power generation technologies [53], since they include not only the cost of the components (photovoltaic modules, batteries, etc.) but also that of the power electronics and grid connection systems (inverters and switchboards), as well as measurement and protection devices and grid connection costs [54,55].

Fig. 4 shows the yearly power forecast of one single PV module considering Plodio's coordinates, a tilt of 14° and south facing (azimuth of 0°). The yearly operation of the module accounts for approximately 1280 EOH. Fig. 5 shows the yearly power forecast of one ENERCON-E40 wind turbine (rated power of 500 kW) determined as a function of the turbine power curve and wind speed data in the hills surrounding the municipality.

Table 1
User annual load data.

User	F1 [kWh]	F2 [kWh]	F3 [kWh]
M1	1255	3359	6050
M2	849	872	1605
M3	1607	1564	3299
M4	1819	1841	3078
RPV1	1095	1120	1571
RPV2	715	776	1010
R1	233	493	432
R2	270	178	328
R3	480	576	741
R4	381	425	622
R5	410	530	680

Regarding grid interaction, a time-dependent price of buying electricity was defined, since prices are normally higher during periods of peak consumption. A buying price of 350 €/MWh was set for time periods inside the F1 band. Instead, for time periods outside this band, the buying price was reduced by approximately 12.5 %. The selling price of electricity was set at 200 €/MWh. It is important to mention that a precise estimation of such prices represents a difficult task, especially in the current European energy scenario, where the energy crisis causes volatile prices within the market, increasing their forecasting uncertainty. An overview of the electricity price data used for the simulations is provided in Table 3. Note that the combination of the feed-in premium incentive and the return of grid tariffs is applied to the total shared energy within the community, as defined in (53). Different prices are specified for the main simulation scenarios and the sensitivity analysis, as explained in the following subsections.

The user interaction with the grid involves indirect CO_2 emissions, since the Italian electrical mix is not only made by RES but also fossil fuel generators, such as gas turbines that use natural gas as the primary energy source and steam power plants fed by coal [56]. To estimate the indirect carbon dioxide emissions related to purchasing electricity, the Italian grid emission factor was used, accounting for 0.216 $kgCO_2/kWh$ [57].

4.2. Case study main results

To address the planning of a REC from different perspectives, several scenarios were analyzed while changing some key attributes of the model, as presented in Table 4. The main optimal scenario (A) considers the minimization of TAC with user selection as a decision variable, with a conservative price of selling electricity. Scenario B also includes the minimization of TAC but forcing the model to include all the users in the REC. The other two scenarios consider the maximization of the shared energy within the REC as an objective. Scenario C analyses the case where only PV and BESS are included as resources while scenario D also includes the modelling of wind turbines.

All the reported scenarios can be compared with a reference case, where users do not join to form an energy community. This case is used to set a reference cost value that regards electricity bills and a reference CO_2 emission. Notice that the reference case is not a static one, since it depends on the users that would be selected in the optimal case. As an example, if the model chooses only four municipality users out of the eleven possible users, the reference case should consider only the same 4 municipality users, but without including REC's technologies. Nevertheless, considering the case where all the 11 users are included, then total annual costs regarding electricity bills are 11850 €, and total annual CO_2 emissions are 7966 kg.

Computational times for different scenarios were recorded to assess the efficiency of the proposed optimization model. The optimization was run on a computer featuring a Processor Intel(R) Core(TM) i7–8565U CPU @ 1.80 GHz and 16 GB of installed RAM. For the TAC scenarios, optimization runs required between 6 and 14 minutes to complete. Conversely, for the scenarios that maximize the shared energy, the computational time increased significantly, reaching approximately 120 minutes. This increase in computational time is likely due to the introduction of binary variables needed to linearize Eq. (46).

4.2.1. Minimization of TAC

Table 5 shows the selected users and installed technologies for scenario A, i.e., "TAC $p^{el,s}$ 0.2". It is noted that only five users are chosen to participate in the REC, three municipality and two residential ones, where all of them have their maximum available PV capacity installed, totalizing approximately 290 kW of installed PV capacity. Moreover, BESS and wind turbines are not installed, mainly due to their high capital costs.

Table 2
User technologies input data.

User	Roof tilt [°]	Roof azimuth 1 [°]	Roof azimuth 2 [°]	$A_{u,1}^{PV,max}$ [m^2]	$A_{u,2}^{PV,max}$ [m^2]	$N_u^{BESS,max}$
M1	10	−94	86	280	280	5
M2	15	−90	90	275	420	5
M3	20	15	1607	63	-	5
M4	15	0	1819	80	-	5
RPV1	25	8.7	1095	69	-	5
RPV2	25	21.4	715	37	-	5

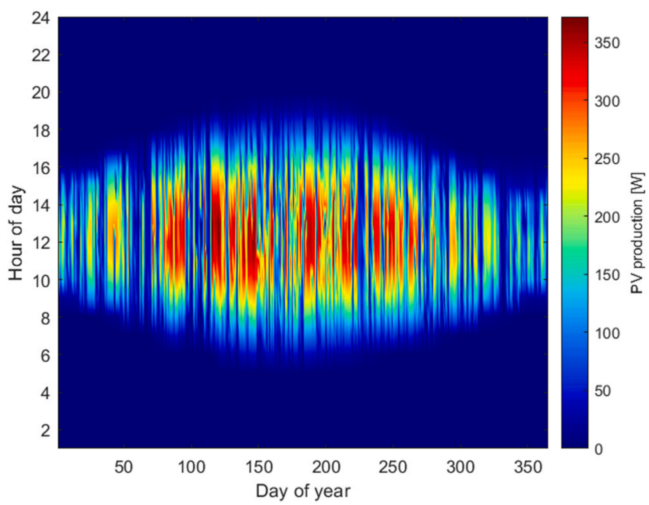

Fig. 4. PV module yearly production.

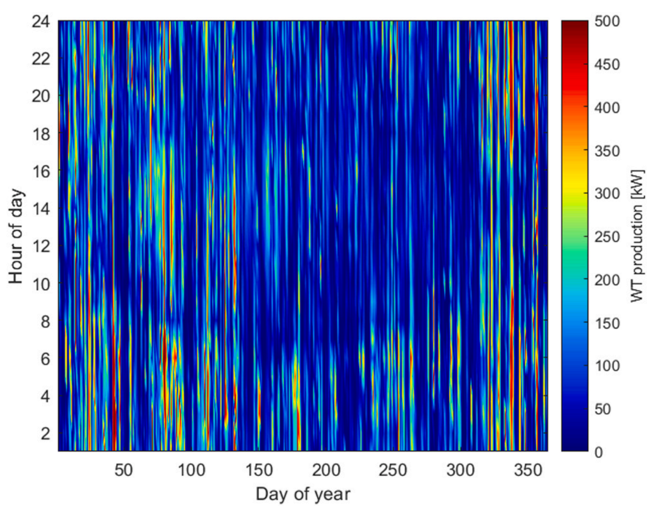

Fig. 5. Wind turbine yearly production.

Table 3
Overview of electricity prices data.

Simulation type	Buying price [€/MWh]	Selling price [€/MWh]	Feed-in premium [€/MWh]	Return of grid tariffs [€/MWh]
Main scenarios	350	200	110	8.37
Sensitivity analysis on prices	400	300	110	8.37

Table 4
Simulated scenarios.

Scenario	Objective function	User selection	Wind turbines modelling	Selling price [€/MWh]
TAC $p^{el,s}$ 0.2 (A)	Total annualized costs	Optimal	Yes	200
TAC $p^{el,s}$ 0.2 ALL (B)	Total annualized costs	All users	Yes	200
E^{sh} $p^{el,s}$ 0.2 (C)	Shared energy	Optimal	No	200
E^{sh} $p^{el,s}$ 0.2 WT (D)	Shared energy	Optimal	Yes	200

The model chooses the five users for some reasons:

- M1 and M2 are the users with larger available surface area, therefore they can install PV for feeding their load and then selling surplus power to the grid.
- Although M4 does not have a large available surface area, its PV plant was already installed, thus it does not imply capital costs but only operational ones.
- RPV1 and RPV2 are residential users with relatively large available solar resources when compared to their small load consumption. Therefore, they can sell a considerable amount of their surplus renewable energy to the grid.

Regarding the PV systems operation (i.e., their EOH), the one installed in RPV1 presents the best performance because it has the finest module's orientation, since modules are almost perfectly south oriented and with a tilt of 25°.

Fig. 6 presents the annual electrical balance for each of the five selected users. M1 and M2 have the largest part of their RES production targeted to sales, due to their large installed PV plants, whereas M3 has its production evenly distributed between selling power, buying power and auto consumption. RPV1 and RPV2 present the same electricity distribution observed in M1 and M2, but with a lower magnitude.

Table 6 shows the cost-related results obtained from the optimization of the two TAC scenarios. As mentioned before, scenario A is characterized by high production and export of renewable electricity, which is also highlighted by the high selling revenues, i.e., 66325 €. Very large savings are also achieved due to the high sales revenues, which make the $OPEX^{total}$ in Eq. (56) highly negative. However, although this case has a good profitability and a reasonable payback period (8.7 years), most of the revenues are concentrated in renewable electricity sales and not sharing. In fact, Table 7 shows that the actual percentage of shared energy that is indirectly used to supply consumption is only 2.05 %, and almost negligible when compared to the overall production (i.e., 0.14 %).

Table 8 shows the installed technologies for scenario B, where TAC is minimized again but with the model forcing all users to participate to the REC. The main difference between the previous case and this one is

Table 5
Selected users and installed technologies for scenario A.

User	U_u^{user}	N_u^{PV}	$N_u^{PV,\max}$	PV Size [kW]	EOH_u^{PV} [h]	N_u^{BESS}	$N_u^{BESS,\max}$	BESS Size [kWh]	Total CAPEX [€]	OPEX [€]
M1	1	290	290	116	1168	0	5	0	232000	1740
M2	1	360	360	144	1148	0	5	0	288000	2160
M3	0	0	32	0	0	0	5	0	0	0
M4	1	20	20	8	1280	0	5	0	0	120
RPV1	1	35	35	14	1304	0	5	0	28000	210
RPV2	1	19	19	7.6	1283	0	5	0	15200	114

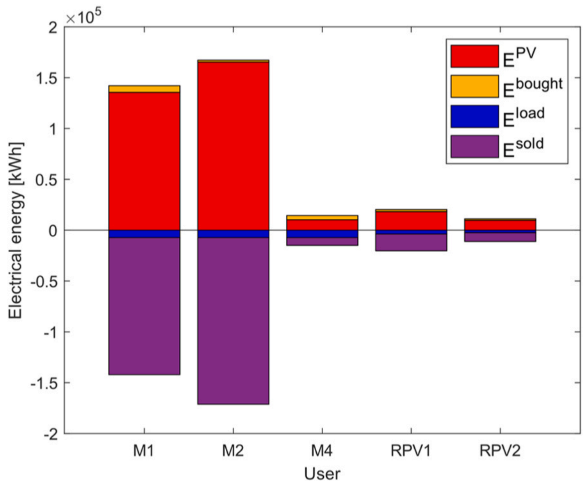

Fig. 6. Annual electrical balance for users in scenario A.

that now a new 12.8 kW PV plant is installed with the inclusion of M3 in the community. This inclusion is carried out by the model to increase revenues, now that all users must participate in the community (even those who are not prosumers). In this case, the total installed PV power reaches 302.4 kW.

Fig. 7 presents the annual electrical balance of the REC for scenario B. The distribution of energy flows is similar to the one reported in case A, where most of the produced energy is exported, although in this case conventional users are also added, which slightly increases the overall electricity demand of the community. Table 7 shows that the percentage of energy shared over the consumed one increases five-fold with respect to scenario A, nonetheless, it is still a small amount since it totalizes only 10 % of the overall demand. One of the reasons is the fact that many of the load profiles, such as the residential ones, have higher or peak values during the evening, when there is no production of energy and thus, no injection of energy into the grid.

It is also noted that even though all users are included in scenario B, its KPIs are not so different from case A and sometimes even slightly better. For example, scenario A has a more negative TAC but a slightly lower SPBT than scenario B. In general, scenario B represents an interesting solution since it has better energy sharing indicators and it can include more users. Also, its economic performance is comparable to the one of case A. However, both cases A and B are defined by low sharing of energy inside the REC and high injection of renewable electricity into the distribution grid. The last one can be a problem if we analyze the impact of the proposed REC from a grid point of view, as it might raise the stress on the grid instead of relieving it, increasing the challenge of managing power flows by transmission and distribution system operators (TSOs and DSOs). However, it also introduces the positive effect of providing clean electricity to the grid, contributing to the reduction of its emission factor, since the REC is acting as an aggregated solar power plant. Both scenarios A and B have relevant CO_2 emissions reductions (31.49 % and 26.78 %), due to their high PV installed capacity.

4.2.2. Maximization of shared energy

Table 9 shows the selected users and installed technologies for scenario C. All the users are chosen to be members of the REC. Moreover, differently from the TAC scenarios, PV modules are not installed on all

Table 6
Cost-related results for scenarios A and B.

Scenario	N° of users	TAC [€]	Total CAPEX [€]	Total OPEX [€]	Benefit [€]	Selling revenues [€]	Savings [%]	SPBT [y]
TAC $p^{el,s}$ 0.2 (A)	5	−12981	563200	−56980	57.30	66325	855	8.7
TAC $p^{el,s}$ 0.2 ALL (B)	11	−10516	588800	−56139	436.59	69127	577	8.6

Table 7
Energy-related results for scenarios A and B.

Scenario	E^{sh} [kWh]	E^{sh} over consumption [%]	E^{sh} over production [%]	CO_2 reduction [%]	Demand [kWh]	E^{PV} [kWh]
TAC $p^{el,s}$ 0.2 (A)	484	2.05	0.14	31.49	23631	339066
TAC $p^{el,s}$ 0.2 ALL (B)	3688	10	1.04	26.78	36880	355513

Table 8
Installed technologies for scenario B.

User	U_u^{user}	N_u^{PV}	$N_u^{PV,\max}$	PV Size [kW]	EOH_u^{PV} [h]	N_u^{BESS}	$N_u^{BESS,\max}$	BESS Size [kWh]	Total CAPEX [€]	OPEX [€]
M1	1	290	290	116	1168	0	5	0	232000	1740
M2	1	360	360	144	1148	0	5	0	288000	2160
M3	1	32	32	12.8	1285	0	5	0	25600	192
M4	1	20	20	8	1280	0	5	0	0	120
RPV1	1	35	35	14	1304	0	5	0	28000	210
RPV2	1	19	19	7.6	1283	0	5	0	15200	114
R1-R5	1	0	0	0	0	0	0	0	0	0

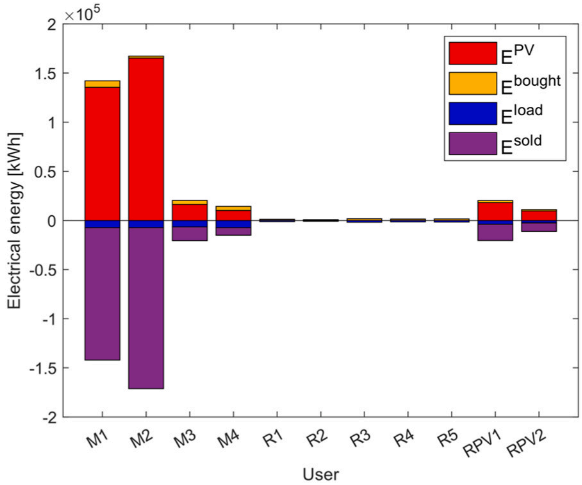

Fig. 7. Annual electrical balance for users in scenario B.

the available surface for each user. The total installed PV capacity is approximately 204 kW, which is 86 kW lower than the one in scenario A and 98.4 kW lower than scenario B. This shows that the installed PV capacity can be considerably lower than the maximum allowed one in order to maximize the shared energy inside the community.

Furthermore, BESS technologies are chosen to be installed for users M1 and M2, summing 72 kWh of available storage capacity. Batteries are chosen since they can provide flexibility by storing renewable electricity produced during the day and using it during the night, either by feeding the loads directly or by injecting it into the grid. This injection of energy during the night can be used to feed indirectly the loads of the other users, increasing the amount of shared energy. In fact, Fig. 8 captures this behavior, where it is noted that both M1 and M2 use their batteries to store solar energy during the day and provide it during the night. Moreover, the discharging of BESS allows a peak in the shared energy during the evening, approximately at 20:00.

Table 10 presents the cost-related results for scenarios C and D. Regarding scenario C, TAC are less negative than A and B and the SPBT is higher (i.e., 10 years), since now the selling revenues are lower and capital costs are higher due to the BESS (approximately 4.4 M€). Although there is a higher benefit due to the sharing of energy, it is not sufficient to compensate for the higher total CAPEX.

The percentage of the shared energy over the total consumption increases significantly when compared to cost minimization scenarios, as seen in Table 11. Approximately 67 % of the community's demand is indirectly supplied by solar power generated inside of it, and this shared energy represents 10.48 % of the overall energy produced. These indicators show that scenario C is characterized by a higher local consumption of the energy that is produced in the community itself, consequently reducing the dependence on the transmission grid.

Scenario D differs from C because it includes wind turbines in the mathematical model. Table 12 shows that the optimization model chooses two 500 kW wind turbines, reaching the maximum allowed limit of 1 MW for a REC's plant. The introduction of such technologies

Table 9
Selected users and installed technologies for scenario C.

User	U_u^{user}	N_u^{PV}	$N_u^{PV,\max}$	PV Size [kW]	EOH_u^{PV} [h]	N_u^{BESS}	$N_u^{BESS,\max}$	BESS Size [kWh]	Total CAPEX [€]	OPEX [€]
M1	1	271	290	108	1168	5	5	36	242000	1986
M2	1	219	360	88	1129	5	5	36	200400	1674
M3	1	0	32	0	0	0	5	0	0	0
M4	1	20	20	8	1280	0	5	0	0	120
RPV1	1	0	35	0	0	0	5	0	0	0
RPV2	1	0	19	0	0	0	5	0	0	0
R1-R5	1	0	0	0	0	0	0	0	0	0

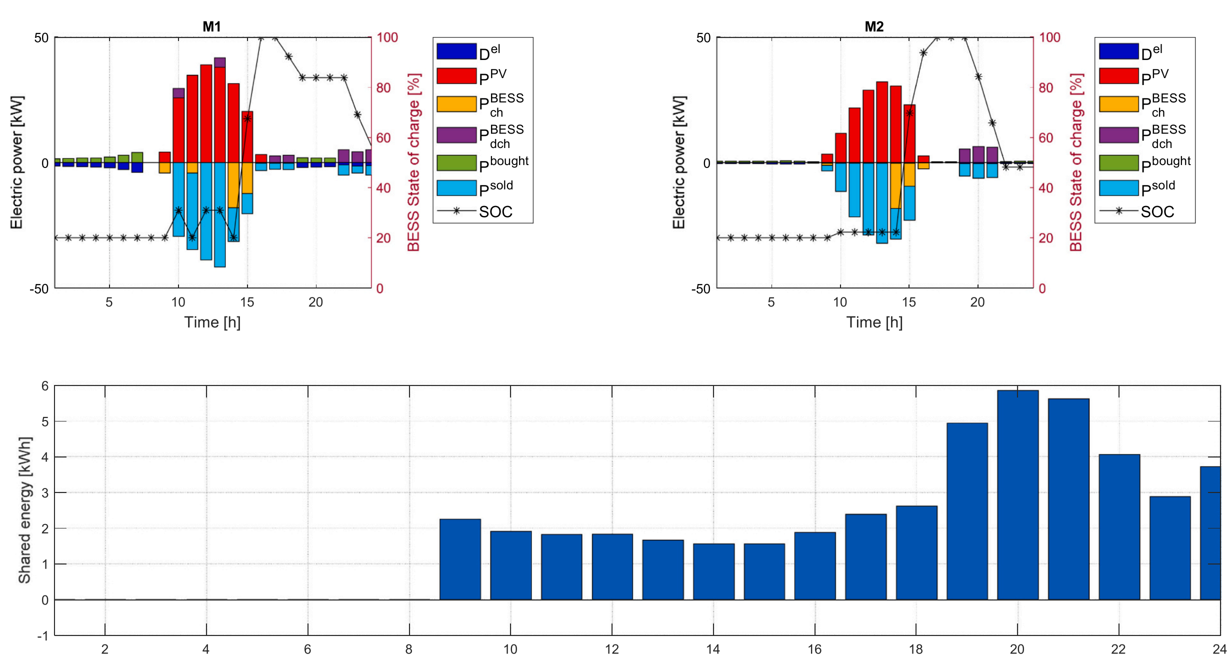

Fig. 8. Electrical dispatch of M1 (top left) and M2 (top right) technologies, and shared energy (bottom) in a winter day.

Table 10
Cost-related results for scenarios C and D.

Scenario	N° of users	TAC [€]	Total CAPEX [€]	Total OPEX [€]	Benefit [€]	Selling revenues [€]	Savings [%]	SPBT [y]
E^{sh} $p^{el,s}$ 0.2 (C)	11	−6069	442400	−41923	2926.8	45222	478	10.5
E^{sh} $p^{el,s}$ 0.2 WT (D)	11	44077	3477600	−225370	3840.2	336812	2034	14.4

Table 11
Energy-related results for scenarios C and D.

Scenario	E^{sh} [kWh]	E^{sh} over consumption [%]	E^{sh} over production [%]	CO_2 reduction [%]	Demand [kWh]	E^{PV} [kWh]
E^{sh} $p^{el,s}$ 0.2 (C)	24726	67.04	10.48	20.12	36880	235825
E^{sh} $p^{el,s}$ 0.2 WT (D)	32443	87.97	1.92	11.48	36880	25663

Table 12
Installed WT in scenario D.

WT model	N° of WT	Size [kW]	EOH^{WT} [h]	Total CAPEX [€]	OPEX [€]
E−40	2	1000	1663	3400000	100000

substantially increases the amount of shared energy inside the energy community. The percentage of shared energy over the consumption is approximately 88 % since, differently from the solar resource, wind is present also during the non-sunshine hours, when a large part of the REC's electrical loads is concentrated. However, when the shared energy is compared to the overall energy produced, a much lower percentage is obtained (i.e., 1.92 %), since the size of the installed turbines is very large compared to the REC's loads.

The selected users and installed technologies for scenario D can be seen in Table 13. Less PV modules are installed with respect to scenario C, but the storage capacity remains the same. The low installed capacity of PV power (i.e., 21.6 kW) is due to the almost redundancy of these technologies when large size generators, such as the two 500 kW WTs, are installed. Fig. 9 illustrates this aspect by showing the difference between the order of magnitude of the energy produced by the turbines and the shared energy, at each timestep. For example, taking as sample the relatively small wind production near the 80th hour of the week, which represents almost 30 kWh, and comparing it to the community's aggregated loads at the same period, which correspond to 8.3 kWh, it is possible to notice that even when the wind resource is low it is almost always higher than the aggregated community consumption. Therefore, the last one almost always defines the shared energy profile in this case.

Overall, scenarios C and D show that is possible to increase the shared energy in the community by using less PV modules, including storage technologies and wind turbines. However, the two last technologies significantly increase capital and operational costs, resulting in increased pay back periods: 10.5 years for scenario C and 14.4 years for scenario D. Moreover, wind turbine installation and maintenance are much more complex than for photovoltaic modules, requiring large financial and organizational resources. These aspects must be considered when planning the configuration of a REC.

4.3. Sensitivity analysis

Two main features of the optimization model were chosen to be subject of a sensitivity analysis:

- Electricity prices: The previous section presented results contemplating more conservative energy prices than the current ones. For instance, the average price of electricity in the market, i.e., *Prezzo Unico Nazionale* (PUN), in the month of August of 2022 was 543.15 €/MWh [58], and this price does not take into account the taxes present in conventional electricity bills. Therefore, there is a possibility of increasing buying and selling prices of electricity to consider a scenario where the prices will remain high in the future.
- Users: The potential REC described in the present paper regards mainly municipality and residential users, that present lower electrical consumptions during the period between morning and afternoon, when there is PV power production. A sensitivity analysis can be performed including a user that has consistent load profile during the day, such as an industrial one, to understand how it affects the sharing of energy inside the energy community when the objective function seeks to maximize it.

4.3.1. Variation of electricity prices

To consider a scenario with higher electricity prices, the peak value of buying electricity was increased to 400 €/MWh and the selling price of electricity was increased to 300 €/MWh.

Table 14 reports the selected users and the installed technologies for the first sensitivity analysis (S1). All the users who can install PV systems are chosen to participate in the REC and they install the maximum allowed PV capacity on their roofs. Moreover, differently from the other cost-optimized scenarios, the sensitivity S1 includes the installation of two 500 kW wind turbines, the same as in scenario D. This occurs since now there is a higher selling price of electricity and the investment in such technologies results in higher profits.

Table 15 and Table 16 show cost and energy related results. It is interesting to note that total annualized cost is much more negative than in previous scenarios, indicating higher profitability. As discussed before, the presence of wind turbines increases the amount of shared energy inside the REC, representing an advantage over scenarios A and

Table 13
Selected users and installed technologies for scenario D.

User	U_u^{user}	N_u^{PV}	$N_u^{PV,\max}$	PV Size [kW]	EOH_u^{PV} [h]	N_u^{BESS}	$N_u^{BESS,\max}$	BESS Size [kWh]	Total CAPEX [€]	OPEX [€]
M1	1	4	290	1.6	1174	5	5	36	28400	384
M2	1	30	360	12	1129	5	5	36	49200	540
M3	1	0	32	0	0	0	5	0	0	0
M4	1	20	20	8	1280	0	5	0	0	120
RPV1	1	0	35	0	0	0	5	0	0	0
RPV2	1	0	19	0	0	0	5	0	0	0
R1-R5	1	0	0	0	0	0	0	0	0	0

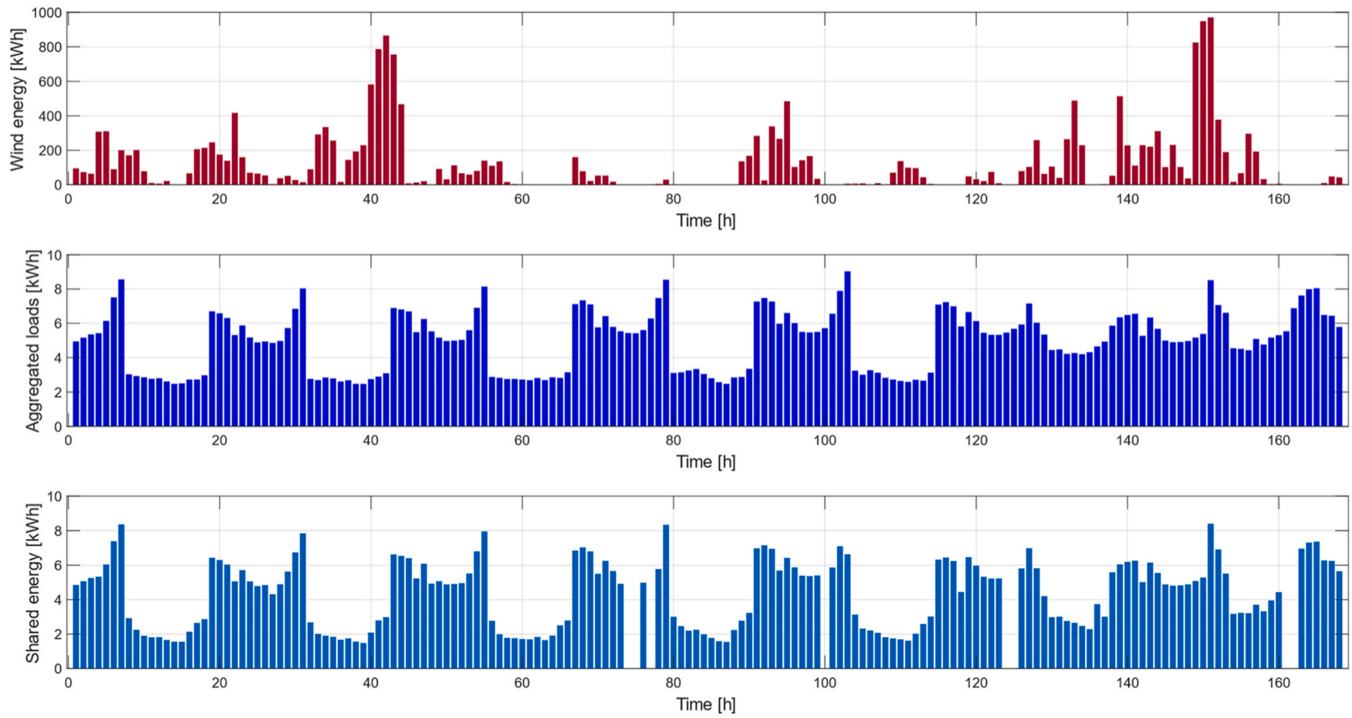

Fig. 9. Wind power production and shared energy over a winter week in scenario D.

Table 14
Selected users and installed technologies for sensitivity S1.

User	U_u^{user}	N_u^{PV}	$N_u^{PV,\max}$	PV Size [kW]	EOH_u^{PV} [h]	N_u^{BESS}	$N_u^{BESS,\max}$	BESS Size [kWh]	Total CAPEX [€]	OPEX [€]
M1	1	290	290	116	1168	0	5	0	232000	1740
M2	1	360	360	144	1148	0	5	0	288000	2160
M3	1	32	32	12.8	1285	0	5	0	25600	192
M4	1	20	20	8	1280	0	5	0	0	120
RPV1	1	35	35	14	1304	0	5	0	28000	210
RPV2	1	19	19	7.6	1283	0	5	0	15200	114

Table 15
Cost-related results for sensitivity S1.

Scenario	N° of users	TAC [€]	Total CAPEX [€]	Total OPEX [€]	Benefit [€]	Selling revenues [€]	Savings [%]	SPBT [y]
TAC $p^{el,s}$ 0.3 (S1)	6	−181069	3988800	−490966	2134.6	602640	4574	7.9

Table 16
Energy-related results for sensitivity S1.

Scenario	E^{sh} [kWh]	E^{sh} over consumption [%]	E^{sh} over production [%]	CO_2 reduction [%]	Demand [kWh]	E^{PV} [kWh]
TAC $p^{el,s}$ 0.3 (S1)	18033	59.90	0.89	32.81	30101	355513

B, which are characterized by much lower values of shared energy. However, the shared energy is still lower than in scenarios C and D, mainly because these cases have higher overall electrical demand (more users) and also the installation of storage technologies. A higher electrical demand increases the overall energy absorbed by the users ($E_t^{grid,b}$). Similarly, battery storage systems help increasing the simultaneity between the energy consumed by the users and the energy produced inside the REC ($E_t^{grid,s}$).

4.3.2. Inclusion of an industrial user

The sensitivity S2 case is defined by the introduction of an industrial user as a potential member of the REC, in order to assess the difference in terms of shared energy inside the community. Such user is a real industry, which operates in the food sector. The facility is characterized by approximately 1 MW of contracted power, and its load profile was estimated considering a reference industrial profile. Since industrial facilities operate almost constantly, their load profile is much more regular, especially between morning and evening.

The selected users and installed technologies for sensitivity S2 are reported in Table 17. All the available surfaces from residential and municipality users are used for installing PV modules. However, although the industrial user is selected as member of the community, the model does not choose to install any PV modules on its very large roof. This occurs since the objective function is set to maximize the REC's shared energy, and thus the presence of PV modules connected to the

Table 17
Selected users and installed technologies for sensitivity S2.

User	U_u^{user}	N_u^{PV}	$N_u^{PV,\max}$	PV Size [kW]	EOH_u^{PV} [h]	N_u^{BESS}	$N_u^{BESS,\max}$	BESS Size [kWh]	Total CAPEX [€]	OPEX [€]
M1	1	290	290	116	1168	5	5	36	257200	2100
M2	1	360	360	144	1148	5	5	36	313200	2520
M3	1	32	32	12.8	1285	0	5	0	25600	192
M4	1	20	20	8	1280	0	5	0	0	120
RPV1	1	35	35	14	1304	0	5	0	28000	210
RPV2	1	19	19	7.6	1283	0	5	0	15200	114
R1-R5	1	0	0	0	0	0	0	0	0	0
IND	1	0	9346	0	0	0	0	0	0	0

industry's POD would most likely decrease the shared energy, since the power locally produced would be mainly used for self-consumption, and the value of $E_t^{grid,b}$ in (46) would be lower.

As in the previous sensitivity case (S1) two 500 kW wind turbines are installed. In fact, as shown in Table 18, the effect of high wind energy production and the very high load absorption of the industrial user leads to an exponential increase of the shared energy when compared to the previous scenarios, reaching a value of approximately 1.67 GWh. This value represents 82.72 % of the total renewable electricity, meaning that a very high share of the REC's production is used to indirectly feed the industrial loads.

Fig. 10 illustrates the relationship between the overall RES production, the industrial loads and the shared energy inside the REC, considering a summer week. The ensamble of PV plants installed in the REC acts in an aggregated way so that, together with the wind turbines, a large amount of power can be injected into the grid. Since the industrial user is characterized by a very high continuous absorption of power from the grid, the result is that the overall shared energy is quite high.

Notice that the shape of the shared energy profile is very similar to the overall RES production one, since according to Eq. 46 the shared energy is the minimum between the injected and absorbed energy, and in this case the injected one is almost always the lower one. This explains also the not so high percentage of shared energy over the total consumption, i.e., 35.16 %. Also, the high absorption of power coming from the industrial user makes CO_2 emissions reduction achieved through the self-consumption of PV power by the prosumers almost negligible. This is because the definition of CO_2 emissions reduction used in this work does not include the positive effect of energy sharing in lowering the emissions.

5. Conclusion

Renewable energy communities (RECs) and their legal definition in the EU are recent topics that are being carefully studied in academia. However, there is still a gap in the scientific literature regarding REC's optimal planning in terms of energy technologies and user participation. Many of the studies presented in the literature approach the subject not considering a high temporal resolution nor a more detailed model of solar photovoltaics power forecasting. Also, the problem is normally only analyzed from an economic perspective, where either the total annualized cost or net present value is used as the objective function. This paper proposes a full-year MILP optimization model that focuses on the aforementioned features, with particular attention to PV power modelling. The model includes up to two different roof orientations, characterized by their tilt and azimuth, to make it compatible with the realistic construction characteristics of buildings. A high temporal resolution is guaranteed by simulating one year with an hourly timestep. A particularly interesting feature is that the model allows the selection of the best group of users in the REC, according to the chosen objective by the introduction of a binary decision variable. This property can be very useful in the study of RECs with a very large number of potential users.

Two different perspectives are analyzed by defining a cost-related objective function and an energy-related one. One objective focuses on minimizing TAC, while the other objective aims to maximize the amount of shared energy within the REC. This objective function is interesting with respect to a possible future scenario where shared energy incentives are higher than the current energy prices. In order to define a practical case study, the municipality of Plodio, located in the northwest of Italy, was chosen to host a potential REC. A total of 11 users, including residential and municipality ones, were considered as possible members of the community. Four different scenarios and two sensitivity analyses were established to analyse the influence of different objective functions, electricity prices and user types.

The obtained results showed that:

- When the minimization of TAC is considered, the model selects only users that have an available surface for the installation of PV modules, since they can provide revenues to the REC by selling a substantial amount of renewable electricity. Instead, conventional residential users (without PV) would contribute negatively to the community's TAC since the costs of their electricity bills are higher than the benefit obtained by their contribution on the shared energy inside the REC. However, it is noted that by forcing their inclusion in the community, the obtained results do not present very different economic KPI's with respect to the optimal selection case.
- When the maximization of shared energy is considered, the model selects all the users, since a larger electrical demand is present in this case. A lower number of PV modules is installed when compared to the cases where TAC is minimized. Technologies such as wind turbines and electrical batteries are exploited to increase flexibility and therefore the number of time periods characterized by injection of renewable electricity in the grid. However, since these technologies have high capital and operational costs, the economic KPIs are quite different than those obtained in the cost-optimized scenarios. The payback period increases from approximately 8.6 years in the cost-optimized scenarios to either 10.5 years or 14.4 years in the maximization of shared energy scenarios, depending on whether wind turbines are included or not in the mathematical model. The higher values of shared energy indicate that there is a higher indirect consumption of the energy that is locally produced inside the REC, representing a positive effect since it can help reduce the stress and dependence on the transmission network.
- The increase of electricity prices increases the profitability of the investment. This happens since there are higher avoided costs related

Table 18
Energy-related results for sensitivity S2.

Scenario	E^{sh} [kWh]	E^{sh} over consumption [%]	E^{sh} over production [%]	CO_2 reduction [%]	Demand [kWh]	E^{PV} [kWh]
TAC $p^{el,s}$ 0.3 (S1)	1669868	35.16	82.72	0.21	4749088	355513

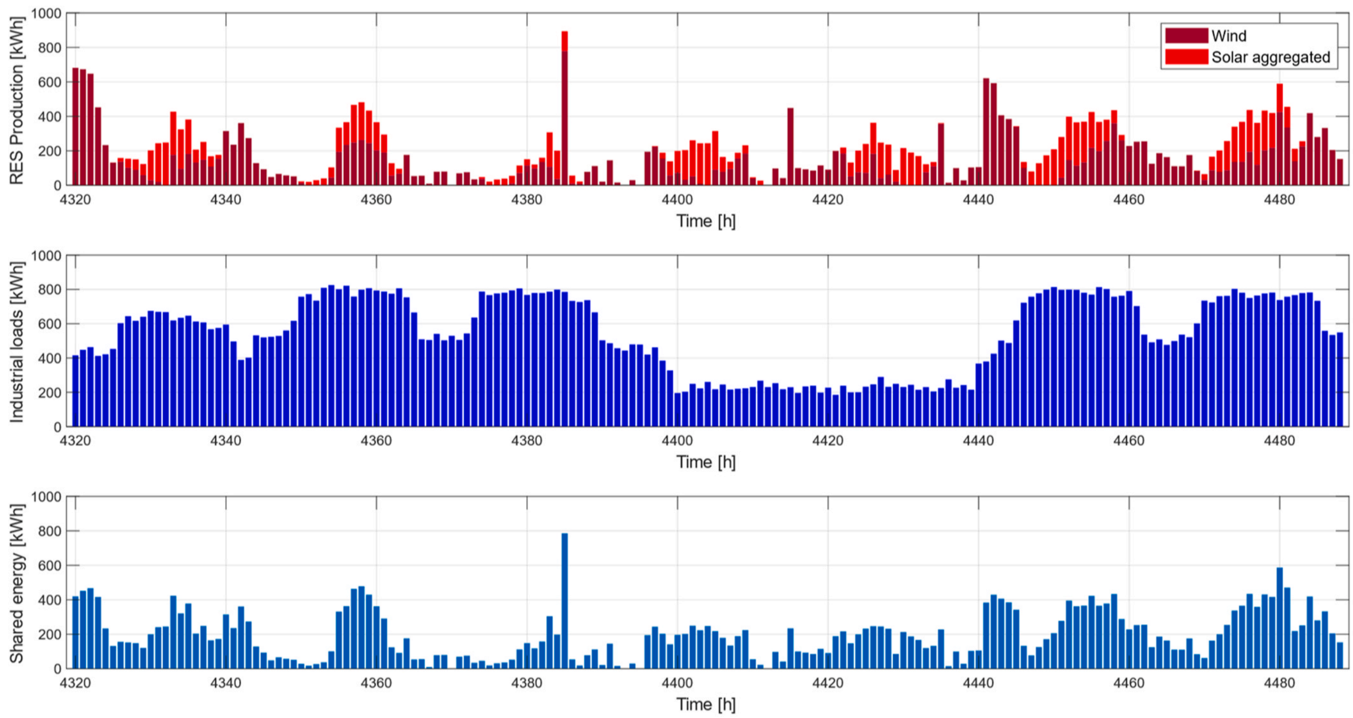

Fig. 10. RES production, Industrial loads and shared energy over a summer week in sensitivity S2.

to the electricity bills and higher profits related to the selling of the surplus energy produced.

- The inclusion of a new user type, defined by an industrial facility, changes dramatically the results related to the sharing of energy in the REC. Because this user is characterized by a more consistent load profile and a very high demand, thus, a very large share of the surplus renewable electricity injected into the distribution grid is defined as shared energy. This share is defined as 82.72 % of the overall renewable production, representing the highest value among the other scenarios.

In general, the results showed that although optimized cost scenarios are more profitable, they are defined by much less shared energy than their counterparts. On the other hand, better energy-sharing indicators are achieved when the decentralized production of renewable energy has a similar magnitude to the community's aggregated demand. These aspects should be taken into account by energy planners, investors, and policymakers, since the implementation of a REC involves not only economic aspects but also environmental and grid-related issues.

It is worth mentioning that a limitation of the proposed case study is that, even though real monthly bills in Italy are used as input for the load profile generation, reference profiles from another country are utilized to fit the monthly consumption values. As stated, this was due to the lack of historical data from residential households and public buildings, given the recent introduction of smart meters. This should improve in the coming years, as more buildings in Italy adopt smart metering technology.

Although the proposed model presents interesting results regarding a REC's planning, there are further future analyses that could be performed to better understand the effects of introducing the following features: modelling of load shifting, other user types (such as commercial ones, hospitals, etc), the inclusion of thermal energy technologies (e.g., heat pumps), consideration of user-dependent energy prices, and fair distribution of benefits among the users.

CRediT authorship contribution statement

Barbara Bonvini: Writing – review & editing, Writing – original draft, Methodology, Conceptualization. **Stefano Bracco:** Writing – review & editing, Writing – original draft, Supervision, Methodology, Conceptualization. **Bruno Laurini:** Writing – review & editing, Writing – original draft, Software, Methodology, Conceptualization.

Declaration of Competing Interest

The authors declare that they have no known competing financial interests or personal relationships that could have appeared to influence the work reported in this paper.

Acknowledgement

The authors would like to thank the Mayor of the Plodio municipality, Dr. Gabriele Badano, for providing data and valuable insights regarding the definition of possible community members.

Data availability

The data that has been used is confidential.

References

[1] G. Bianco, B. Bonvini, S. Bracco, F. Delfino, P. Laiolo, G. Piazza, Key performance indicators for an energy community based on sustainable technologies, Sustainability 13 (2021) 8789.

[2] European Commission, Directorate-General for Energy. (2019). Clean energy for all Europeans. Publications Office. Retrieved from ⟨https://data.europa.eu/doi/10.2833/9937⟩.

[3] Renewable Energy Directive 2018/2001/EU. (2018). Retrieved from ⟨https://eur-lex.europa.eu/legal-content/EN/TXT/?uri=uriserv:OJ.L_.2018.328.01.0082.01.ENG&toc=OJ:L:2018:328:TOC⟩.

[4] Eurostat. (2022). EU overachieves 2020 renewable energy target. Retrieved from ⟨https://ec.europa.eu/eurostat/web/products-eurostat-news/-/ddn-20220119-1⟩.

[5] M. De Simon-Martin, S. Bracco, G. Piazza, L.C. Pagnini, A. Gonzalez-Martinez, F. Delfino, The role of energy communities in the energy framework, Springe Appl. Sci. Technol. (2022) 7–29.

[6] Ricerca sul Sistema Energetico – RSE. (2020). Gli schemi di Autoconsumo Collettivo e le Comunità dell'Energia 2020.
[7] P. Esposito, E. Marrasso, C. Martone, G. Pallotta, C. Roselli, M. Sasso, M. Tufo, A roadmap for the implementation of a renewable energy community, Heliyon 10 (2024) e28269.
[8] F. Vecchi, R. Stasi, U. Berardi, Modelling tools for the assessment of Renewable Energy Communities, Energy Rep. 11 (2024) 3941–3962.
[9] P. De Juan-Vela, A. Alic, V. Trovato, Monitoring the Italian transposition of the EU regulation concerning renewable energy communities and the relevant policies for battery storage, J. Clean. Prod. 425 (2023) 138937.
[10] G. Comodi, A. Bartolini, F. Carducci, B. Nagaranjan, A. Romagnoli, Achieving low carbon local energy communities in hot climates by exploiting networks synergies in multi energy systems, Appl. Energy 256 (2019) 113901.
[11] S. Dafoe, M. Krarti, K. Baker, Optimal Designs of Grid-Connected Energy Efficient and Resilient Residential Communities, ASME J. Eng. Sustain. Build. Cities 3 (1) (2022) 011004.
[12] F. Braeuer, M. Kleinebrahm, E. Naber, F. Scheller, R. McKenna, Optimal system design for energy communities in multi-family buildings: the case of the German Tenant Electricity Law, Appl. Energy 305 (2022) 117884.
[13] M. Cutore, R. Volpe, R. Sgroi, A. Fichera, Energy management and sustainability assessment of renewable energy communities: The Italian context, Energy Convers. Manag. 278 (2023) 116713.
[14] V. Casalicchio, G. Manzolini, M.G. Prina, D. Moser, From investment optimization to fair benefit distribution in renewable energy community modelling, Appl. Energy 310 (2022) 118447.
[15] M. Zatti, M. Moncecchi, M. Gabba, A. Chiesa, F. Bovera, M. Merlo, Energy Communities Design Optimization in the Italian Framework, Appl. Sci. 11 (11) (2021) 5218.
[16] A. Cosic, M. Stadler, M. Mansoor, M. Zellinger, Mixed-integer linear programming based optimization strategies for renewable energy communities, Energy 237 (2021) 121559.
[17] G. Piazza, F. Delfino, S. Bergero, M. Di Somma, G. Graditi, S. Bracco, Economic and environmental optimal design of a multi-vector energy hub feeding a Local Energy Community, Appl. Energy 347 (2023) 121259.
[18] M. Fresia, L. Bordo, F. Delfino, S. Bracco, Optimal day-ahead active and reactive power management for microgrids with high penetration of renewables, Energy Convers. Manag.: X 23 (2024) 100598.
[19] M. Fresia, S. Bracco, Electric vehicle fleet management for a prosumer building with renewable generation, Energies 16 (20) (2023) 7213.
[20] J. Cao, C. Crozier, M. McCulloch, Z. Fan, Optimal design and operation of a low carbon community based multi-energy systems considering EV integration, IEEE Trans. Sustain. Energy 10 (3) (2019) 1217–1226.
[21] G. Piazza, S. Bracco, F. Delfino, S. Siri, Optimal design of electric mobility services for a Local Energy Community, Sustain. Energy, Grids Netw. 26 (2021) 100440.
[22] E. Barabino, D. Fioriti, E. Guerrazzi, I. Mariuzzo, D. Poli, M. Raugi, E. Razaei, E. Schito, D. Thomopulos, Energy Communities: A review on trends, energy system modelling, business models, and optimisation objectives, Sustain. Energy, Grids Netw. 36 (2023) 101187.
[23] J. Sousa, J. Lagarto, C. Camus, C. Viveiros, F. Barata, P. Silva, R. Alegria, O. Paraiba, Renewable energy communities optimal design supported by an optimization model for investment in PV/wind capacity and renewable electricity sharing, Energy 283 (2023) 128464.
[24] A. Dimovski, M. Moncecchi, M. Merlo, Impact of energy communities on the distribution network: An Italian case study, Sustain. Energy, Grids Netw. 35 (2023) 101148.
[25] T. Weckesser, D.F. Dominković, E.M. Blomgren, A. Schledorn, H. Madsen, Renewable Energy Communities: Optimal sizing and distribution grid impact of photo-voltaics and battery storage, Appl. Energy *301* (2021) 117408, https://doi.org/10.1016/j.apenergy.2021.117408.
[26] B. Velkovski, V.Z. Gjorgievski, D. Kothona, A.S. Bouhouras, S. Cundeva, N. Markovska, Impact of tariff structures on energy community and grid operational parameters, Sustain. Energy, Grids Netw. 38 (2024) 101382, https://doi.org/10.1016/j.segan.2024.101382.
[27] N. Tomin, V. Shakirov, A. Kozlov, D. Sidorov, V. Kurbatsky, C. Rehtanz, E.E. Lora, Design and optimal energy management of community microgrids with flexible renewable energy sources, Renew. Energy 183 (2022) 903–921, https://doi.org/10.1016/j.renene.2021.11.024.
[28] R. Sudhoff, R. Derzbach, S. Schreck, S. Thiem, S. Niessen, On the operation and implications of grid-interactive renewable energy communities, Sustain. Energy, Grids Netw. 38 (2024) 101390, https://doi.org/10.1016/j.segan.2024.101390.
[29] F. Lazzari, G. Mor, J. Cipriano, F. Solsona, D. Chemisana, D. Guericke, Optimizing planning and operation of renewable energy communities with genetic algorithms, Appl. Energy 338 (2023) 120906, https://doi.org/10.1016/j.apenergy.2023.120906.
[30] G. Volpato, G. Carraro, M. Cont, P. Danieli, S. Rech, A. Lazzaretto, General guidelines for the optimal economic aggregation of prosumers in energy communities, Energy 258 (2022) 124800, https://doi.org/10.1016/j.energy.2022.124800.
[31] P. Mehta, V. Tiefenbeck, Solar PV sharing in urban energy communities: Impact of community configurations on profitability, autonomy and the electric grid, Sustain. Cities Soc. 87 (2022) 104178, https://doi.org/10.1016/j.scs.2022.104178.
[32] M.S. Simoiu, I. Fagarasan, S. Ploix, V. Calofir, Modeling the energy community members' willingness to change their behaviour with multi-agent systems: A stochastic approach, Renew. Energy 194 (2022) 1233–1246, https://doi.org/10.1016/j.renene.2022.06.004.
[33] E. Dal Cin, G. Carraro, G. Volpato, A. Lazzaretto, P. Danieli, A multi-criteria approach to optimize the design-operation of Energy Communities considering economic-environmental objectives and demand side management, Energy Convers. Manag. 263 (2022) 115677, https://doi.org/10.1016/j.enconman.2022.115677.
[34] M. Krug, M.R. Di Nucci, L. Schwarz, I. Alonso, I. Azevedo, M. Bastiani, A. Dyląg, E. Laes, A. Hinsch, G. Klāvs, et al., Implementing European Union Provisions and Enabling Frameworks for Renewable Energy Communities in Nine Countries: Progress, Delays, and Gaps, Sustainability 15 (11) (2023) 8861.
[35] Gestore dei servizi energetici – GSE. (2022). Regole tecniche per l'accesso al servizio di valorizzazione e incentivazione dell'energia elettrica condivisa..
[36] Löfberg, J. (2004). A toolbox for modeling and optimization in MATLAB. Proceedings of the CACSD Conference, 284-289.
[37] Gurobi Optimization LLC. (2022). Gurobi Optimizer Reference Manual. Retrieved from ⟨https://www.gurobi.com⟩.
[38] Autorità di Regolazione per Energia Reti e Ambiente - ARERA. (2021). *Glossario della bolletta per la fornitura di energia elettrica*.
[39] Hybrid Optimization of Multiple Energy Resources – HOMER. (n.d.). Load Profile Menu. Retrieved from ⟨https://www.homerenergy.com/products/pro/docs/latest/load_profile_menu.html⟩.
[40] J.A. Duffie, W.A. Beckman, Solar Engineering of Thermal Processes, John Wiley & Sons, 2013.
[41] S.A. Kalogirou, Solar Energy Engineering: Processes and Systems, Academic Press, 2013.
[42] T. Huld, R. Müller, A. Gambardella, A new solar radiation database for estimating PV performance in Europe and Africa, Sol. Energy 86 (2012) 1803–1815.
[43] M. Mattei, G. Notton, C. Cristofari, M. Muselli, P. Poggi, Calculation of the polycrystalline PV module temperature using a simple method of energy balance, Renew. Energy 31 (4) (2006) 553–567. ISSN 0960-1481.
[44] Marion, Anderberg, A., Deline, C., Glick, S.H., Muller, M., Perrin, G., Rodriguez, J., Rummel, S., Terwilliger, K., Silverman, T.J. (2014). User's Manual for Data for Validating Models for PV Module Performance.
[45] Marion, Bill, Anderberg, Allan, Deline, Chris, Muller, Matthew, Perrin, Greg, Rodriguez, Jose, Rummel, Steve, Silverman, Timothy, Vignola, Frank, Barkaszi, Stephen. (2014). Data for Validating Models for PV Module Performance. United States.
[46] Vaishali Sohoni, S. Gupta, Rajesh Nema, A Critical Review on Wind Turbine Power Curve Modelling Techniques and Their Applications in Wind Based Energy Systems, J. Energy 2016 (2016) 1–18.
[47] S. Araveti, C.A. Quintana, E. Kairisa, A. Mutule, J.P.S. Adriazola, C. Sweeney, P. Carroll, Wind energy assessment for renewable energy communities, Wind 2 (2022) 325–347.
[48] Ricerca sul Sistema Energetico – RSE. (n.d.). Wind Atlas. Retrieved from ⟨http://atlanteeolico.rse-web.it⟩.
[49] J.F. Manwell, J.G. McGowan, A.L. Rogers, Wind energy explained: theory, design and application, John Wiley & Sons, 2010.
[50] S. Bracco, F. Delfino, A. Trucco, S. Zin, Electrical storage systems based on Sodium/Nickel chloride batteries: A mathematical model for the cell electrical parameter evaluation validated on a real smart microgrid application, J. Power Sources 399 (2018) 372–382.
[51] Istituto Nazionale di Statistica - ISTAT, Bilancio demografico anno 2022, 2022.
[52] National Renewable Energy Laboratory (NREL). (2021). End-Use Load Profiles for the U.S. Building Stock [data set]. Retrieved from https://dx.doi.org/10.25984/1876417.
[53] IRENA, Renewable Power Generation Costs in 2019 (2020).
[54] Khorrami, S., Khazaee, M., Roldán-Fernández, J.M., & Martirano, L. (2024, March). Cost-benefit Analysis of PV Self-Consumption in Residential Sector in Italy. In 2024 11th Iranian Conference on Renewable Energy and Distribution Generation (ICREDG) (Vol. 11, pp. 1-8). IEEE.
[55] P. Lazzeroni, F. Moretti, F. Stirano, Economic potential of PV for Italian residential end-users, Energy 200 (2020) 117508.
[56] International Energy Agency, Electricity generation by source, 2020, IEA, Italy, 2020.
[57] European Environment Agency, Greenhouse gas emission intensity of electricity generation, 2020, EEA, 2020.
[58] Gestore dei Mercati Energetici (GME). (2022). Average PUN in August 2022. Retrieved from ⟨https://www.mercatoelettrico.org/it/Statistiche/ME/DatiSintesi.aspx⟩.